AD-A072 850 FORD AEROSPACE AND COMMUNICATIONS CORP NEWPORT BEACH --ETC F/G 4/1
METHOD OF CALCULATING H20 TRANSMISSION BETWEEN 333 AND 633 CM-1--ETC(U)
APR 79 D E BURCH, D A GRYVNAK F19628-76-C-0302
UNCLASSIFIED U6503 AFGL-TR-79-0054 NL

1 OF 1
AD A072 850

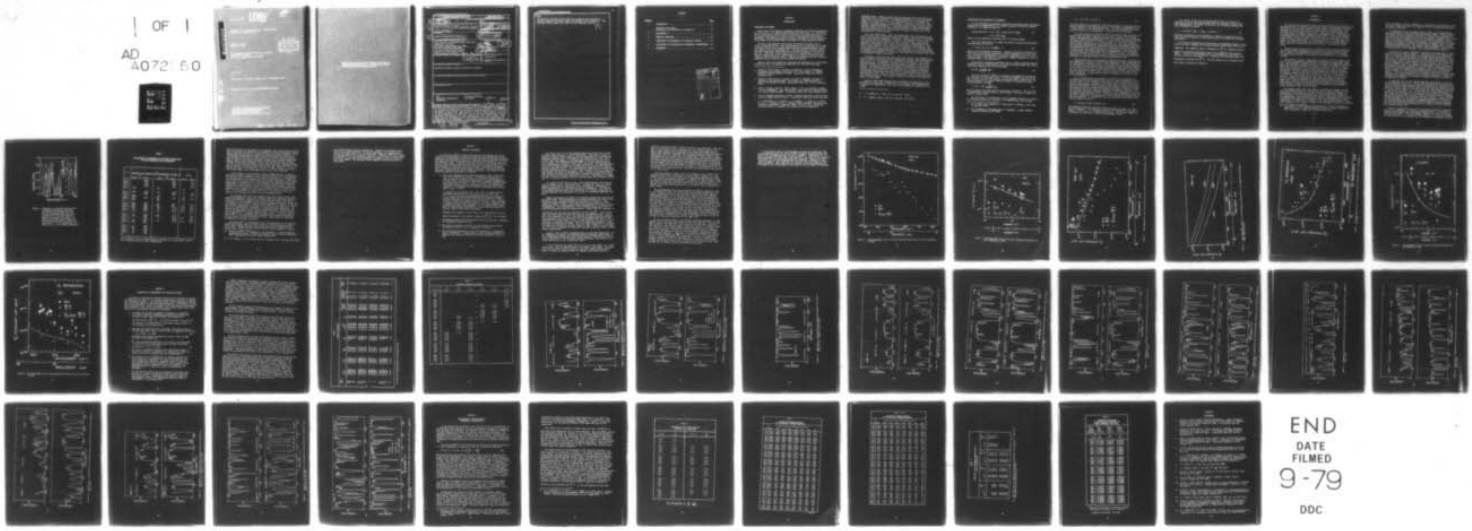

END
DATE FILMED
9-79
DDC

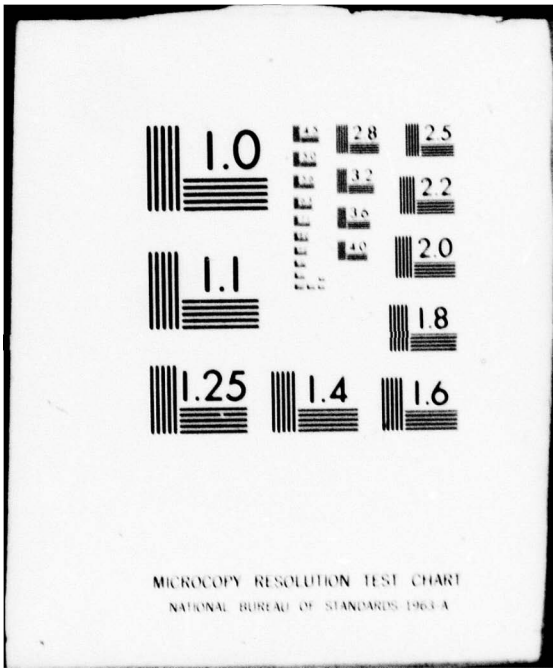
1.0
1.1
1.25
1.4
1.6
1.8
2.0
2.2
2.5
2.8
MICROCOPY RESOLUTION TEST CHART
NATIONAL BUREAU OF STANDARDS 1963 A

AFGL-TR-79-0224

LEVEL II

# METHOD OF CALCULATING $H_2O$ TRANSMISSION BETWEEN 333 and 633 $cm^{-1}$


Russell E. Burch
David K. Gryvnak

Ford Aerospace and Communications Corporation
Aeronutronic Division
Ford Road, Newport Beach, CA 92663




April 1979

Final Report for Period 4 October 1976 - 30 September 1978

Approved for public release; distribution unlimited


AIR FORCE GEOPHYSICS LABORATORY
AIR FORCE SYSTEMS COMMAND

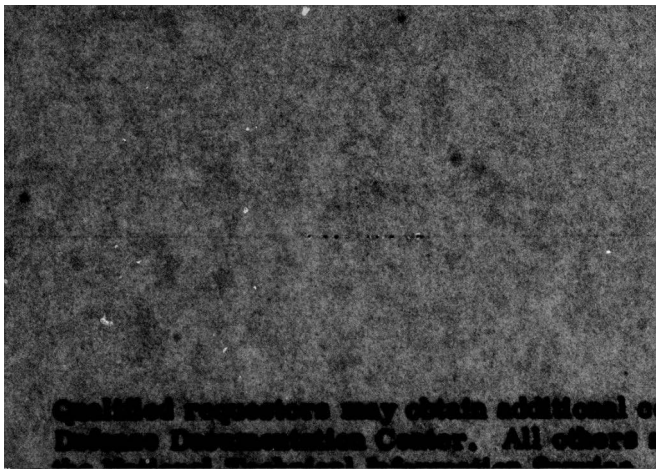

SECURITY CLASSIFICATION OF THIS PAGE (When Data Entered)

# REPORT DOCUMENTATION PAGE

READ INSTRUCTIONS BEFORE COMPLETING FORM

| | |
|---|---|
| 1. REPORT NUMBER: AFGL-TR-79-0054 | 2. GOVT ACCESSION NO. |
| 3. RECIPIENT'S CATALOG NUMBER | |
| 4. TITLE (and Subtitle): Method of Calculating $H_2O$ Transmission Between 333 and 633 $cm^{-1}$ | 5. TYPE OF REPORT & PERIOD COVERED: Final Report. 4 Oct 76 - 30 Sep 78 |
| 6. PERFORMING ORG. REPORT NUMBER: U6503 | |
| 7. AUTHOR(s): Darrell E. Burch, David A. Gryvnak | 8. CONTRACT OR GRANT NUMBER(s): F19628-76-C-0302 |
| 9. PERFORMING ORGANIZATION NAME AND ADDRESS: Ford Aerospace and Communications Corporation, Aeronutronic Division, Ford Road, Newport Beach, CA 92663 | 10. PROGRAM ELEMENT, PROJECT, TASK AREA & WORK UNIT NUMBERS: 7670 / 09 |
| 11. CONTROLLING OFFICE NAME AND ADDRESS: Air Force Geophysics Laboratories, Hanscom AFB, Massachusetts 01731, Contract Monitor: Anthony P. D'Agati OPI | 12. REPORT DATE: Apr 79; NUMBER OF PAGES: 50 |
| 14. MONITORING AGENCY NAME & ADDRESS (if different from Controlling Office) | 15. SECURITY CLASS. (of this report): Unclassified |
| | 15a. DECLASSIFICATION/DOWNGRADING SCHEDULE |

16. DISTRIBUTION STATEMENT (of this Report)

Approved for public release; distribution unlimited

17. DISTRIBUTION STATEMENT (of the abstract entered in Block 20, if different from Report)

18. SUPPLEMENTARY NOTES

19. KEY WORDS (Continue on reverse side if necessary and identify by block number)

$H_2O$
Atmospheric Transmission
Absorption
Continuum Absorption
Line Shape

1/333 cm 1/633 cm

20. ABSTRACT (Continue on reverse side if necessary and identify by block number)

Spectral absorption data are presented for $H_2O$ between 333 $cm^{-1}$ and 633 $cm^{-1}$. An empirical continuum has been determined to account for all of the absorption not attributed to absorption lines centered within approximately 30 $cm^{-1}$ of any wavenumber of observation. The empirical continuum, which consists of one part for self broadening of the $H_2O$ lines and one part for $N_2$ broadening, has been determined experimentally for three temperatures: 296K, 338K and 430K. Other values based on extrapolation have been determined for lower temperatures representative of the atmosphere. A line-by-line calculation scheme involving

DD FORM 1 JAN 73 1473 EDITION OF 1 NOV 65 IS OBSOLETE

Unclassified

SECURITY CLASSIFICATION OF THIS PAGE (When Data Entered)

391 853

cont.
20.
the empirical continuum and the AFGL line parameters has been used to calculate spectra for several samples investigated in the laboratory. The calculated spectra agree quite well with the laboratory spectra.

CONTENTS


| Section | | Page |
|---|---|---|
| 1 | INTRODUCTION | 4 |
| | Background and Summary | 4 |
| | Definitions and Discussions of Parameters | 6 |
| 2 | EXPERIMENTAL | 9 |
| 3 | EMPIRICAL CONTINUUM | 15 |
| 4 | COMPARISON OF EXPERIMENTAL AND CALCULATED SPECTRA | 26 |
| 5 | APPLICATION TO CALCULATIONS OF ATMOSPHERIC TRANSMITTANCE | 43 |
| 6 | REFERENCES | 50 |


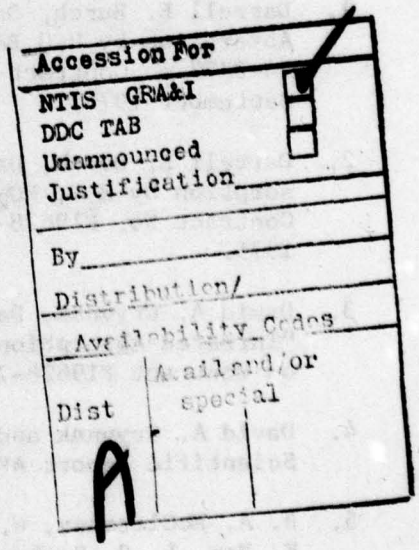

## SECTION 1

## INTRODUCTION

### BACKGROUND AND SUMMARY

Water vapor is the dominant atmospheric absorbing gas between approximately 333 and 633 $cm^{-1}$, the spectral region covered by this report. It is essential that the absorption in this region be sufficiently well understood that it can be calculated accurately for a wide variety of path lengths and atmospheric conditions. This spectral region has certain advantages for remote sensing of the atmosphere from satellite-borne instruments and ground-based instruments.

The water vapor spectrum contains many individual absorption line of widely varying intensities. The average absorption over intervals wide enough to contain several lines increases generally from the high wavenumber side of this region to the low wavenumber side. Previous reports[1-4] from our laboratory show experimental data obtained with laboratory samples of pure $H_2O$ and $H_2O + N_2$. These data include spectral curves of transmittance as well as results of measurements of the transmittance at the centers of several narrow "windows" between absorption lines. Important information about the continuum absorption has been derived from the window measurements.

Spectra based on the AFGL[5] line parameters and calculated by a line-by-line method agree well with experimental data near the relatively strong $H_2O$

---

1. Darrell E. Burch, David A. Grynvak, and Francis J. Gates; "Continuum Absorption by $H_2O$ Between 330 and 825 $cm^{-1}$", Final Report No. AFCRL-TR-74-0377 on Contract F19628-74-C-0069. Aeronutronic Report No. U-6095, September 1974.

2. Darrell E. Burch, David A. Grynvak, and John D. Pembrook; "Infrared Absorption by $H_2O$, $NO_2$ and $N_2O_4$", Final Report No. AFCRL-TR-75-0420 on Contract No. F19628-75-C-0049. Aeronutronic Report No. U-6159, September, 1975.

3. David A. Gryvnak, Darrell E. Burch, Robert L. Alt, and Dorianne K. Zgonc; "Infrared Absorption by $CH_4$, $H_2O$ and $CO_2$", Final Report No. AFGL-TR-76-0246 on Contract F19628-76-C0067. Aeronutronic Report No. U-6275, December 1977.

4. David A. Gryvnak and Darrell E. Burch, "Infrared Absorption by $CO_2$ and $N_2O$." Scientific Report AFGL-TR-78-0154. Aeronutronic Report No. U-6417, May 1978.

5. R. A. McClatchey, W. S. Benedict, S. A. Clough, D. E. Burch, R. F. Calfee K. Fox, L. S. Rothman, and J. S. Garing; "AFCRL Atmospheric Absorption Line Parameters Compilation", AFCRL-TR-73-0096, 26 January 1973. (Associated with this report is a magnetic tape listing the line parameters.)

absorption lines. However, significant discrepancies between the theory and experiment exist at wavenumbers of maximum transmission in the narrow windows several $cm^{-1}$ from strong lines. The discrepancies are more pronounced for samples of pure $H_2O$ than for dilute samples of $H_2O$ in $N_2$. Calculated transmittances are always greater than the observed transmittances in these narrow windows. Palmer[6] and Bignell[7], in previous studies of this spectral region, have also observed that the narrow window absorption is greater for samples with high concentrations of $H_2O$ than would be predicted from spectra of low concentrations of $H_2O$ in the air.

We[4] have demonstrated that the transmittance near the centers of the narrow windows can be calculated accurately by using a line-by-line calculation scheme and including an empirical continuum. Contributions by all of the lines were included in the calculations. Values for the empirical continuum were determined separately for each of the narrow windows. These values, when plotted on a wavenumber scale, could be represented by a smooth curve. This result implies that the "extra" absorption represented by the empirical continuum actually has the characteristics of a continuum; i.e. it changes slowly and smoothly with changing wavenumber. This absorption that is not predictable by the AFGL line parameters is, therefore, not simply due to errors in the widths or intensities of some of the lines.

Sections 3, 4 and 5 of this report deal with a similar, but somewhat different, method of calculation with an empirical continuum. Only lines centered within 30 $cm^{-1}$ of the wavenumber of calculation are included in the line-by-line calculation. An empirical continuum is then determined to make up the difference between the calculated and experimental absorption in the narrow windows. The empirical continuum determined in this manner is presented in Section 3 for self broadening and $N_2$ broadening at 3 different temperatures. Transmittance spectra have been calculated for several samples by a method that includes the empirical continuum and the contributions by the lines centered within 30 $cm^{-1}$. Section 4 shows comparisons of these calculated spectra with laboratory spectra. The agreement between the calculated and laboratory spectra is quite good.

Section 5 deals with extrapolating the empirical continuum data to temperatures lower than those at which data were obtained. This extrapolation is required for application of the data to many atmospheric conditions of interest.

---

6. C. H. Palmer Jr., J. Opt. Soc. Am. 50 1323 (1960)

7. K. J. Bignell, Quart J. Roy. Met. Soc. 96, 390 (1970)

## DEFINITIONS AND DISCUSSION OF PARAMETERS

At the relatively low pressures involved in the present study, the density of $H_2O$ vapor is proportional to its partial pressure p so that the absorber thickness u of a sample is given by

$$u(\text{molecules/cm}^2) = 2.69 \times 10^{19}\ p(\text{atm})\ L(\text{cm})\ (273/\theta) \qquad (1)$$

$$= 7.34 \times 10^{21}\ pL/\theta,$$

where $\theta$ is the temperature in Kelvins and L is the path length.

The true transmittance of a sample that would be observed with infinite resolving power is given by

$$T' = \exp(-u\kappa), \text{ or } (-1/u)\ln T' = \kappa \qquad (2)$$

where $\kappa$ is the absorption coefficient. Because of the finite slitwidth of a spectrometer and possible variations in $\kappa$ with wavenumber due to line structure, the observed transmittance T may differ significantly from T' at the same wavenumber. The quantity T represents a weighted average of T' over the interval passed by the spectrometer.

The intrinsic absorption coefficient due to a single collision-broadened absorption line at a point within a few $cm^{-1}$ of the line center, $\nu_o$, is probably given adequately by the Lorentz shape:

$$k_L = \frac{S}{\pi}\ \frac{\alpha}{(\nu-\nu_o)^2 + \alpha^2}\ . \qquad (3)$$

The line intensity $S = \int k d\nu$ is essentially independent of pressure for the conditions of the present study. It has been shown[8,9] that for $|\nu-\nu_o|$ greater than a few $cm^{-1}$, the Lorentz equation may require modification. One empirical method is to employ a factor $\chi$, which is a function of $(\nu-\nu_o)$, so that Equation 3 becomes

$$k = k_L \chi = \frac{S}{\pi}\ \frac{\alpha\chi}{(\nu-\nu_o)^2 + \alpha^2}\ , \qquad (4)$$

where $k_L$ denotes the value given by the Lorentz coefficient. The value of $\chi$ is approximately equal to unity for small $|\nu-\nu_o|$, but it may be quite different for large $|\nu-\nu_o|$.

The half-width $\alpha$ is proportional to the equivalent pressure, $P_e$, given by the following equation for a mixture of the absorbing gas plus nitrogen.

---

8. D. E. Burch, D. A. Gryvnak, R. R. Patty and C. E. Bartky, J. Opt. Soc., Am. 59, 267 (1969).

9. B. H. Winters, S. Silverman, and W. S. Benedict, J. Quant. Spectry Radiative Transfer 4, 527 (1964).

$$P_e = B_p + p_N = (B-1)p + P. \quad (5)$$

The total pressure is denoted by P, the partial pressure of $N_2$ by $p_N$, and the partial pressure of the absorbing gas by p. Note that $P_e$ approximates P for a dilute mixture of the absorbing gas in $N_2$. The value of B has been determined previously to be approximately 5 for $H_2O$ as the absorbing gas.

The wing absorption coefficient C due to the extreme wings ($|\nu-\nu_o| \gg \alpha$) of several lines is equal to the sum of all of the k's due to the individual lines. Wing absorption changes very slowly with wavenumber and is, therefore, frequently called continuum absorption. It can be seen from Equation (3) that the absorption coefficient at a given wavenumber in the wing of a single Lorentz-shaped absorption line is proportional to $\alpha$. This same proportionality has been experimentally[9] demonstrated both for Lorentz-shaped lines and for non-Lorentz lines that are given by an expression similar to Equation (4). It follows that the continuum absorption coefficient due to the sum of the contributions by the wings of many lines is proportional to the individual $\alpha$'s and is therefore proportional to the equivalent pressure. By combining Equations (1), (2) and (3), it can also be shown that the wing absorption by pure $H_2O$ in a fixed path length is directly proportional to $p^2$.

Dimers consisting of two temporarily joined $H_2O$ molecules ( $H_2O$:$H_2O$) have been suggested as a source of $H_2O$ continuum absorption. Dimer absorption has the same pressure dependence ($p^2L$) as wing absorption by pure $H_2O$; therefore, it is difficult to distinguish which is the source of $H_2O$ continuum absorption. It is certain that much of the continuum absorption discussed in this report is due to the extreme wings of lines because of the proximity of strong lines. Our data alone are not sufficient to prove or disprove the presence of any dimer absorption. We have treated the $H_2O$ continuum as if it were all due to wing absorption.

In the present study, the continuum is studied by investigating the absorption at selected wavenumbers where there is little absorption by lines centered within 1 $cm^{-1}$. However, as discussed in more detail below, there may be a small amount of absorption due to these nearby ($|\nu-\nu_o| < 1$ $cm^{-1}$) lines, and their contribution to the attenuation coefficient is denoted as $\kappa$(local). This quantity may vary rapidly with changing wavenumber as indicated by Equation (3) and, because of collision broadening, it depends on pressure. For the relatively low sample pressures employed, the line halfwidth $\alpha$ of any of the lines is much less than 1 $cm^{-1}$. Therefore, the contributions by any line for which $|\nu-\nu_o| > 1$ $cm^{-1}$ is proportional to $\alpha$ and follows the pressure dependence of continuum. It follows that the total absorption coefficient $\kappa$ for a pure $H_2O$ sample is given by

$$\kappa = \kappa(\text{local}) + C_s^o p = \kappa(\text{local}) + C_s \quad (6)$$

The normalized continuum coefficient $C_s^o$ is the value of $C_s$ when p = 1 atm at a given temperature. The subscript s denotes self broadening of the lines. Since $\alpha_s = \alpha_s^o p$, and u is proportional to pL, it follows that ($-\ln T$) for continuum due to the wings of lines is proportional to $p^2L$.

In a mixture of $H_2O + N_2$, the $H_2O$ absorption lines are broadened by collisions of the absorbing $H_2O$ molecules with $N_2$ molecules as well as with other $H_2O$ molecules. To account for the $H_2O$ - $N_2$ collisions, Equation (6) must be modified as follows

$$\alpha = \alpha(\text{local}) + C_s^o p + C_N^o p_N = \alpha(\text{local}) + C \qquad (7)$$

The small contribution to the absorption by $\alpha$(local) is accounted for as a first step in the reduction of the absorption data to determine the continuum coefficients.

As a means of simplifying the calculation of transmittance spectra, we have divided the self broadening and nitrogen broadening coefficients each into two components. One component, which is disignated as $\sum_{1}^{30} a_k$, represents approximately the calculated contribution by all of the absorption lines centered within $\pm$ 30 $cm^{-1}$ of the wavenumber where the calculation is being made. An empirical continuum, designated by $^aC$, represents the difference between the experimental continuum and $\sum_{1}^{30} a_k$. The exact method used to determine these two factors is discussed in Section 3.

## SECTION 2

## EXPERIMENTAL

The experimental data presented here have been obtained with the grating spectrometer and two adjustable multiple-pass sample cells described previously[10]. The longer of the two cells is used for path lengths of 123 meters or greater; a shorter cell with a base length of 1 meter serves for shorter paths. Essentially all of the optical path outside of the sample cell is confined to two vacuum tanks to eliminate absorption by atmospheric gases. When operating at wavenumbers greater than approximately 430 $cm^{-1}$ ($\lambda \simeq 23.2$ μm) the radiant energy source is a Nernst glower, the sample cell windows are KBr, and a KBr window is used on the detector. At lower wavenumbers, the energy source is a Globar, the sample cell windows are polyethylene, and the detector window is KRS-5. The Ge:Cu sensitive element of the detector is cooled with liquid helium.

Radiant energy from the source is chopped at 450 Hz to permit amplification and synchronous demodulation of the electrical signal from the detector. The dc output of the synchronous demodulator is proportional to the amount of chopped energy incident on the detector and is displayed on a strip-chart recorder.

The pressure of $H_2O$ in a pure sample is measured by an oil manometer that can be read to approximately 0.00003 atm for pressures less than about 0.005 atm. The uncertainty is probably between 0.5% and 1% for higher $H_2O$ pressures. Before the spectrum is scanned or before $N_2$ is added to a sample, the pure $H_2O$ is kept in the cell for several minutes in order for most of the adsorption on the cell walls to occur and the pressure of the vapor to approach equilibrium. The time required to reach equilibrium is sometimes shortened by allowing a sample of pure $H_2O$ to remain in the cell for a few minutes at a pressure 10% - 20% greater than that desired. The extra vapor is then removed by partially evacuating the cell. Partial pressures of $H_2O$ in the $H_2O + N_2$ mixtures are measured by a dew-point meter mounted inside the sample cell. Values of $H_2O$ partial pressure obtained with the dew-point meter agree quite well with the partial pressure measured by the manometer before the $N_2$ is added if sufficient time is allowed for the absorption to reach equilibrium before the $N_2$ is added.

The samples studied cover wide ranges of optical path lengths, temperatures, $H_2O$ partial pressures, and total pressures of $H_2O + N_2$ mixtures. Unfortunately, no data have been obtained at reduced temperatures because of the limitations on the maximum $H_2O$ partial pressure that can be achieved at low temperatures. Data covering the wide range of temperatures make it possible to determine the temperature dependence so that some extrapolation to lower temperatures is probably valid. Samples of pure $H_2O$ have been studied so that self broadening of the absorption lines can be investigated without the influence

10. D. E. Burch, " Investigation of the Absorption of Infrared Radiation by Atmospheric Gases." Semi-Annual Technical Report, Contract F19628-69-C-0263. Aeronutronic Report No. U-4784, January 1970.

of $N_2$ broadening. The $N_2$ broadening of the $H_2O$ lines is determined by comparing the absorption by $H_2O + N_2$ samples with the corresponding absorption by samples of $H_2O$ only.

A "background" curve is scanned with the sample cell evacuated either immediately before or after the sample spectrum is scanned. After the curves are checked and edited slightly to account for small drift or spurious deflections, they are digitized and the data are punched on computer cards. Positions of the $H_2O$ line centers as given on the AFGL line parameter tape are used for wavenumber calibration of the spectra. The spectral curve of transmittance for a sample is obtained by comparing the original curve to the corresponding background curve. The computer output includes tables of transmittance and other quantitites of interest versus wavenumber. Spectral plots of transmittance, or of $(-1/u)\ln T$, can be generated by the computer.

A portion of a typical experimental spectrum of pure $H_2O$ vapor is illustrated by the solid curve in Figure 1. The upper curve in the figure represents a calculated spectrum based on the simple Lorentz line shape (Equation (3) ) and the line parameters on the AFGL line parameters tape. Other theoretical line shapes have also been used in similar calculations but none of the shapes result in good agreement between experimental and theoretical spectra throughout the entire spectral interval covered by this report. The spectrum shown in Figure 1 was chosen for illustration because the discrepancy between theory and experiment is great at these low wavenumbers and is greater for pure $H_2O$ samples than for samples of $H_2O + N_2$. An improvement in the accuracy of a calculated spectrum is shown by the dotted curve in Figure 1. This curve was obtained by including an empirical continuum in the calculation in a manner similar to that described in Section 3. Further improvement could apparently be obtained by slightly decreasing the amount of the empirical continuum.

An important part of this study has been the determination of the continuum absorption coefficients. Much information about the continuum absorption was obtained without scanning spectra by measuring the absorption at the centers of several narrow windows, such as at the two points denoted by vertical broken lines in Figure 1. At these points the small amount of absorption by lines centered within 1 $cm^{-1}$ was accounted for, either graphically or by calculating the absorption by the nearby line from the AFGL line parameters. This correction for nearby lines was usually much smaller than the continuum absorption; therefore, the correction need not be accurate. After $\kappa$(local) had been accounted for, the normalized continuum absorption coefficient $C_S^o$ for self-broadening was determined by applying Equations (1), (2) and (6). The normalized continuum absorption coefficient $C_N^o$ for nitrogen broadening was then determined by applying Equation (1), (2) and (7) to data obtained from mixtures of $H_2O + N_2$.

Table 1, repeated here from two of our previous reports[1-4], summarizes much of the experimental continuum data discussed below. At 296K, $C_S^o$ is generally much greater than at the higher temperature, a result that agrees with previous results in other spectral regions. If, as we have assumed, the major portion of the absorption at the wavenumbers investigated for pure

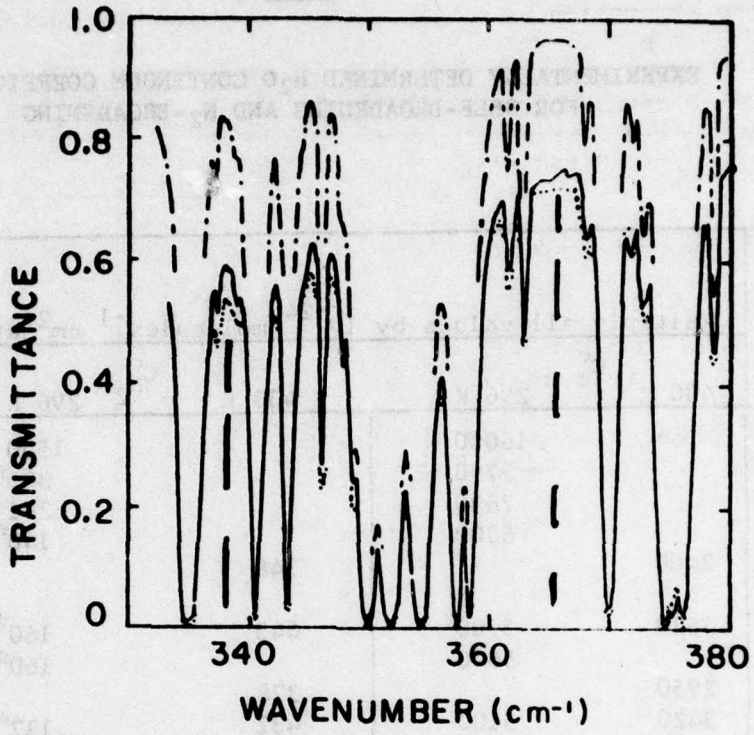


Figure 1. Comparison of calculated spectra with a laboratory spectrum of pure $H_2O$. The solid curve represents the laboratory measurement: the upper curve represents the calculated spectrum based on the Lorentz line shape. An empirical continuum has been added to the calculated spectrum to produce the dotted curve. $P = p = 0.0207$ atm; $\theta = 296$ K, and $u = 1.48 \times 10^{21}$ molecules/cm$^2$.

## TABLE 1

### EXPERIMENTALLY DETERMINED $H_2O$ CONTINUUM COEFFICIENTS FOR SELF-BROADENING AND $N_2$-BROADENING

| $\nu$ $cm^{-1}$ | Multiply all values by $10^{-24}$ molecules$^{-1}$ cm$^2$ atm$^{-1}$ | | | | $C_s^o/C_{N_2}^o$ | |
|---|---|---|---|---|---|---|
| | $C_s^o$ | | $C_{N_2}^o$ | | | |
| | 430 K | 296 K | 430 K | 296 K | 430 K | 296 K |
| 337.9 | | 16000 | | 1530 | | 10.5 |
| 366.0 | | 9790 | | 385* | | 25.4 |
| 389.0 | | 7830 | | 291* | | 26.9 |
| 411.0 | | 6300 | | 140* | | 45.0 |
| 430.0 | 2400 | | 349 | | 6.9 | |
| 433.7 | 4520 | 5700 | 645 | 160** | 7.0 | 35.6 |
| 439.0 | | 5600 | | 160* | | 35.0 |
| 440.1 | 2950 | | 378 | | 7.8 | |
| 448.8 | 3420 | 5100 | 432 | 117* | 7.9 | 43.6 |
| 465.4 | 2320 | | 296 | | 7.8 | |
| 475.1 | 2640 | 4300 | 349 | 157* | 7.6 | 27.4 |
| 482.6 | 2320 | 3950 | 353 | 166* | 6.6 | 23.6 |
| 498.0 | 1200 | 3050 | 110 | 55.3* | 10.9 | 55.2 |
| 531.6 | 762 | 2380 | 62 | 33.6* | 12.3 | 70.8 |
| 559.2 | 573 | 1750 | 44 | 20.2 | 13.1 | 86.6 |
| 579.0 | 972 | 1680 | 138 | 54.7* | | 30.7 |
| 597.0 | 670 | 1500 | 65 | 26.7* | 10.3 | 56.2 |
| 611.4 | | 1170 | | 12.2* | | 95.9 |
| 629.0 | 330 | 1100 | 29 | 13.0* | 13.0 | 84.6 |
| 656.0 | 219 | 1000 | | | | |
| 683.5 | 171 | 930* | | | | |
| 725.5 | 120 | 700* | | | | |
| 764.6 | 97 | 570* | | | | |
| 790.0 | 87 | 540* | | | | |
| 822.0 | 68 | 420* | | | | |

The estimated errors for $C_s^o$ and $C_N^o$ are $\pm$ 5% except for values marked * and ** which indicate $\pm$ 10% and $\pm$ 20%, respectively.

$H_2O$ is due to the extreme wings of the absorption lines, these results indicate that the influence of temperature on the shapes of the self-broadened lines is greater than that predicted by simple theories on collision broadening. This unpredictably strong negative temperature dependence provides a basis for attributing the absorption to dimers because it is known that the concentration of dimers of any molecule decreases rapidly with increasing temperature. However, some of the results shown below in this report, as well as other results of ours shown previously, indicate that the extreme wings of absorption lines have an unpredictably strong negative temperature dependence. This has been observed for $CO_2$ and $N_2O$ as well as for $H_2O$. Therefore, it seems likely that some of the absorption attributed by many to dimers may be due to the extreme wings of lines with shapes that are not well understood.

In all portions of the spectrum, values of $C_s^o/C_N^o$ vary from 5 upwards to much larger numbers, possibly as high as 1000 near 10 $\mu$m.[11,12] The variation in this ratio can be explained on the basis of a difference in the shapes of the extreme wings of $N_2$- broadened and self-broadened $H_2O$ lines. Within about 5 or 10 $cm^{-1}$ of the line centers, both types of lines apparently have similar shapes with the normalized (to 1 atm) halfwidths of self-broadened lines approximately 5 times as great as they are for $N_2$- broadened lines. However, beyond 5 or 10 $cm^{-1}$ from the centers, the absorption by self-broadened lines relative to $N_2$- broadened ones is apparently greater than it is near the centers. This corresponds to a larger value of $\chi$ at a given $|\nu-\nu_o|$ for the wings of self-broadened $H_2O$ lines than for $N_2$-broadened lines.

At wavenumbers where the ratio $C_s^o/C_N^o$ is high, $C_s^o$ decreases rapidly with increasing temperature. This large negative temperature dependence generally cannot be explained by changes in the intensities and widths of the lines. Line widths at 1 atm pressure decrease with increasing temperature, but not at a sufficient rate to account for the observed temperature dependence of $C_s^o$. The most probable explanation is a change in the shapes of the wings of the lines that can be represented by a decrease in $\chi$ with increasing temperature. The largest relative changes in $C_s^o$ occur at wavenumbers where a significant portion of the absorption is due to distant lines. Thus, the relative temperature dependence of $\chi$ increases with increasing $|\nu-\nu_o|$. The results also indicate that $\chi$ for $N_2$-broadened lines decreases with increasing temperature, but at a slower rate than self-broadened lines. This results in a decrease in $C_s^o/C_N^o$ with increasing temperature.

Two other sets[6,7] of experimental data on $H_2O$ absorption in this spectral region also indicate that the relative effect of self-broadening is greater in the narrow windows separated from strong lines than at wavenumbers near strong lines. Neither of these previous studies included samples at tempera-

---

11. Darrell E. Burch, "Investigation of the Absorption of Infrared Radiation by Atmospheric Gases." Semi-Annual Technical Report, Contract F19628-69-C-0263. Aeronutronic Report No. U-4784, January 1970.

12. R. E. Roberts, J. E. A. Selby, and L. M. Biberman, Appl. Opt. 15, 2085 (1976).

tures much different from room temperature. Bignell[7] has published values that can be related directly to our $C_s^o$ and $C_N^o$ within a few wavenumbers of some of the points where we have obtained data. Bignell's sample cell could be operated only at 1 atm pressure; therefore, he was unable to study samples of pure $H_2O$. He studied self-broadening by varying the partial pressure of $H_2O$ in his samples. The agreement between Bignell's data and our data is quite good.

## SECTION 3

## EMPIRICAL CONTINUUM

In a previous report[4], we have shown that the transmittance can be calculated at the wavenumbers of maximum transmittance by a method that involves summing the contributions by all of the lines and adding an empirical continuum. The method used previously includes the calculated contributions by all of the $H_2O$ absorption lines. A similar method has been used to obtain the data presented in this section except that only those lines centered within 30 $cm^{-1}$ of the wavenumber of calculation have been included. An empirical continuum, which is different from the one determined previously[4], has been determined and used in calculating the spectra shown in Section 4. The method of determining the empirical continuum is as follows:

a. One of the temperatures for which experimental values of $C_s^o$ or $C_N^o$ have been determined is selected. The AFGL line parameters are used as input to a computer program to calculate contributions due to these lines at the selected wavenumbers of maximum transmittance. Only those lines for which $1 \leq |\nu-\nu_o| \leq 30$ $cm^{-1}$ are included in the calculation (Recall that the experimental values with which these values are to be compared do not include contributions by lines for which $|\nu-\nu_o| < 1$ $cm^{-1}$).

   In summing the contributions due to the lines, the simple Lorentz line shape (Equation (3)) is used for $|\nu-\nu_o| \leq 20$ $cm^{-1}$. For $20 < |\nu-\nu_o| \leq 30$ $cm^{-1}$, the contribution by each line is given by $k = k_L I$, where $k_L$ corresponds to the Lorentz shape and I varies linearly from unity at $|\nu-\nu_o| = 20$ $cm^{-1}$ to zero at $|\nu-\nu_o| = 30$ $cm^{-1}$. we refer to this as an "apodized bound" of 30 $cm^{-1}$. (The term bound is normally used to denote the value of $|\nu-\nu_o|$ beyond which the contribution by a line is not included.) Use of apodized bound avoids small but undesirable discontinuities in the calculated spectra at a distance equal to bound from strong lines.

   Throughout the remainder of this report, the contribution to the continuum calculated in this manner is denoted as $\sum_1^{30} {}^a k_i^o$. The left-hand superscript denotes the apodized bound, and the superscript o indicates an equivalent pressure of 1 atm.

b. The values calculated in step (a) are substracted from the larger experimental values for the corresponding wavenumbers.

c. The differences calculated in step (b) are plotted on a logarithmic scale vs wavenumber. A smooth curve is drawn through the points to represent the normalized empirical continuum coefficient denoted by ${}^a C_s^o$.

The value of 30 $cm^{-1}$ for the apodized bound was selected after several different values were used in trial calculations. This value is based on a compromise between required computer time and "smoothness" of the resulting empirical continuum curve. For example, the calculated sums of $k^o$ with a 15 $cm^{-1}$ bound were compared at many wavenumbers with sums calculated for a 20 $cm^{-1}$ bound. The differences between these two values contained significant discontinuites at points 15 $cm^{-1}$ from a strong line. The summation based on the 20 $cm^{-1}$ bound included the contribution by this strong line, whereas the other summation did not. The discontinuities observed in the differences between calculations based on a 30 $cm^{-1}$ bound and those based on a larger bound were usually less than the experimental error. Because of the added computer time required, inclusion of contributions by lines centered more than 30 $cm^{-1}$ from the point of calculation would not be justified. Furthermore, the shapes of lines at distances greater than this from the center are not known accurately.

If a normal 30 $cm^{-1}$ bound is used, small discontinuities in the spectra occur at points 30 $cm^{-1}$ from strong lines. In almost all cases, the discontinuity is less than the uncertainty in the calculations. Nevertheless, a small discontinuity in a calculated spectrum is undesirable. By apodizing in the manner described above, the contribution by a distant strong line increases gradually and continuously as the point of calculation approaches the line.

Figure 2 illustrates the method of determining the empirical continuum for pure $H_2O$ at 296K. The solid squares in the figure represent the values of $C_s^o$ obtained from the laboratory measurements discussed in Section 2. These values also appear in Table 1; they correspond to points where most of the absorption is due to lines centered beyond approximately 2 $cm^{-1}$ from the point of measurement. The contributions by lines centered within 1 $cm^{-1}$ have already been substracted from the observed data. Values of $\sum_{1}^{30} a_k^o$ calculated as discussed in step (a) above are represented by the triangles. In all cases, these calculated values are much less than the experimental values. Each of the values represented by the +'s was obtained by substracting the calculated value represented by the triangle from the corresponding experimental value represented by a solid square. Thus, a + sign represents the value of "extra" continuum, or empirical continuum, required to bring about agreement between calculated and experimental values. The curve drawn through the +'s represents the empirical continuum for pure $H_2O$ samples at 296K. Values from this smooth curve are used to represent the empirical continuum coefficient, $^aC_s^o$, in transmission calculations.

Figures 3 and 4 include corresponding data for elevated temperatures. As the temperature increases, the calculated points (triangles) become closer to the corresponding experimental points (solid squares), indicating that the relative contribution by the empirical continuum decreases. (Note that the continuum coefficients are on a logarithmic plot.)

It is of interest that nearly all of the +'s in either Figure 2 or 3 fall within +10% of the corresponding smooth curve based on the points. The deviation from the smooth curve is greater for the 430 K samples represented by Figure 4 because the laboratory data are somewhat less accurate and the

empirical continuum produces a smaller fraction of the absorption. Note that many of the calculated values represented by the triangles would not fall near a single smooth curve. The points that would fall furthest above a smooth curve represent wavenumbers where strong absorption lines are centered within about 3-10 $cm^{-1}$; therefore, the absorption is greater than at other wavenumbers that are further from very strong lines. These points of greater absorption were included to help in providing information about the nature of the "extra" absorption represented by the empirical continuum and about the relative shapes of self-broadened and $N_2$-broadened $H_2O$ lines. It is informative that essentially the same amount of empirical continuum is required to provide agreement between theory and experiment at the wavenumbers of very low absorption as at those points where the calculated absorption coefficient may be 2-5 times greater.

The solid curves of Figure 5 make up a composite of the curves of the normalized coefficients of empirical continuum, $^{a}C_{s}^{o}$, in Figures 2-4. The dashed portions of the curves represent extrapolations discussed in Section 5. The very strong negative temperature dependence of $^{a}C_{s}^{o}$ is obvious. Since the empirical continuum represents the contribution by distant wings of lines, this result strongly supports the argument that the wings decrease in absorption with increasing temperature at a rate greater than is predicted by simple theory.

The corresponding data for $N_2$ broadening are shown in Figures 6,7, and 8. As pointed out above, the distant wings of $N_2$-broadened $H_2O$ lines contribute a smaller fraction of the absorption than do the distant wings of self-broadened lines. It is therefore to be expected that the empirical continuum contribute less for $N_2$-broadenening than for self-broadening. Because of the relatively smaller role played by the empirical continuum for $N_2$ broadening, the accuracy of values determined is less. The experimental data are also less accurate for $N_2$ broadening than for self-broadening. Only a limited number of samples were used to study the $N_2$ broadening at elevated temperatures. Because of the limited data and the smaller part played by the empirical continuum there is more scatter in the data representing the high temperatures than in those for room temperature. No $N_2$ broadening data were obtained at wavenumbers greater than approximately 635 $cm^{-1}$ because of the small effect of adding $N_2$ to a sample of pure $H_2O$ and because of the absorption by unavoidable impurities in the sample cell.

We were not able to measure a significant temperature dependence of $^{a}C_{N}^{o}$ because of the relatively large amount of scatter in the data. The curve for 338K in Figure 7 is identical to the portion of the 296K curve in Figure 6 that covers the same spectral region. Similarly, the curve for 430K in Figure 8 is identical to the corresponding portion of the 296K curve in Figure 6. The curves in Figures 7 and 8 do not represent exactly the best statistical fits to the data points, but the data do not indicate a significant trend with changing temperature. Therefore, in calculations discussed in Sections 4 and 5, we have assumed that $^{a}C_{N}^{o}$ is the same for all of the temperatures covered. Because the empirical continuum due to nitrogen broadening contributes relatively little to total attenuation, errors of several percent in $^{a}C_{N}^{o}$ may contribute little to the errors in the calculated average transmittance over a spectral interval containing several lines.

If the distant wings of self-broadened $H_2O$ lines were shaped the same as $N_2$-broadening lines, the curve for ${}^aC_S^o$ in Figure 2 would be shaped the same as the corresponding curve for ${}^aC_N^o$ in Figure 6. Furthermore, at any given wavenumber, the ratio ${}^aC_S^o$ : ${}^aC_N^o$ would be 5, the ratio of the normalized halfwidths, $\alpha^o$, for self-broadening and $N_2$ broadening. Comparison of the curves in Figures 2 and 6 indicate that the ratio may be as large as 100 at some wavenumbers. This large ratio is evidence of the great difference in the shapes of the extreme wings of the lines for the two types of broadening.

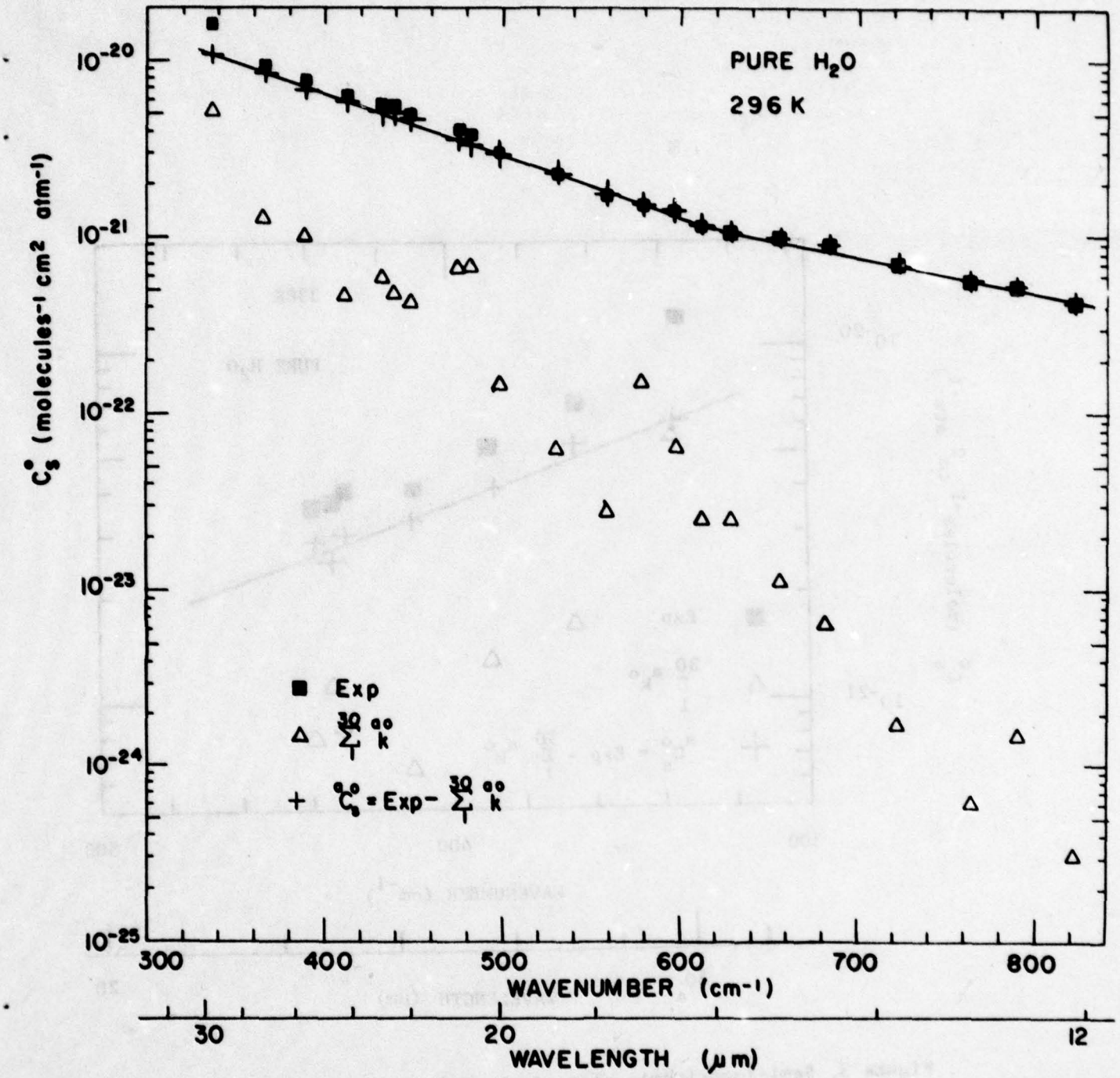


Figure 2. Semi-logarithmic plot of the $H_2O$ continuum coefficient for self broadening at 296K.

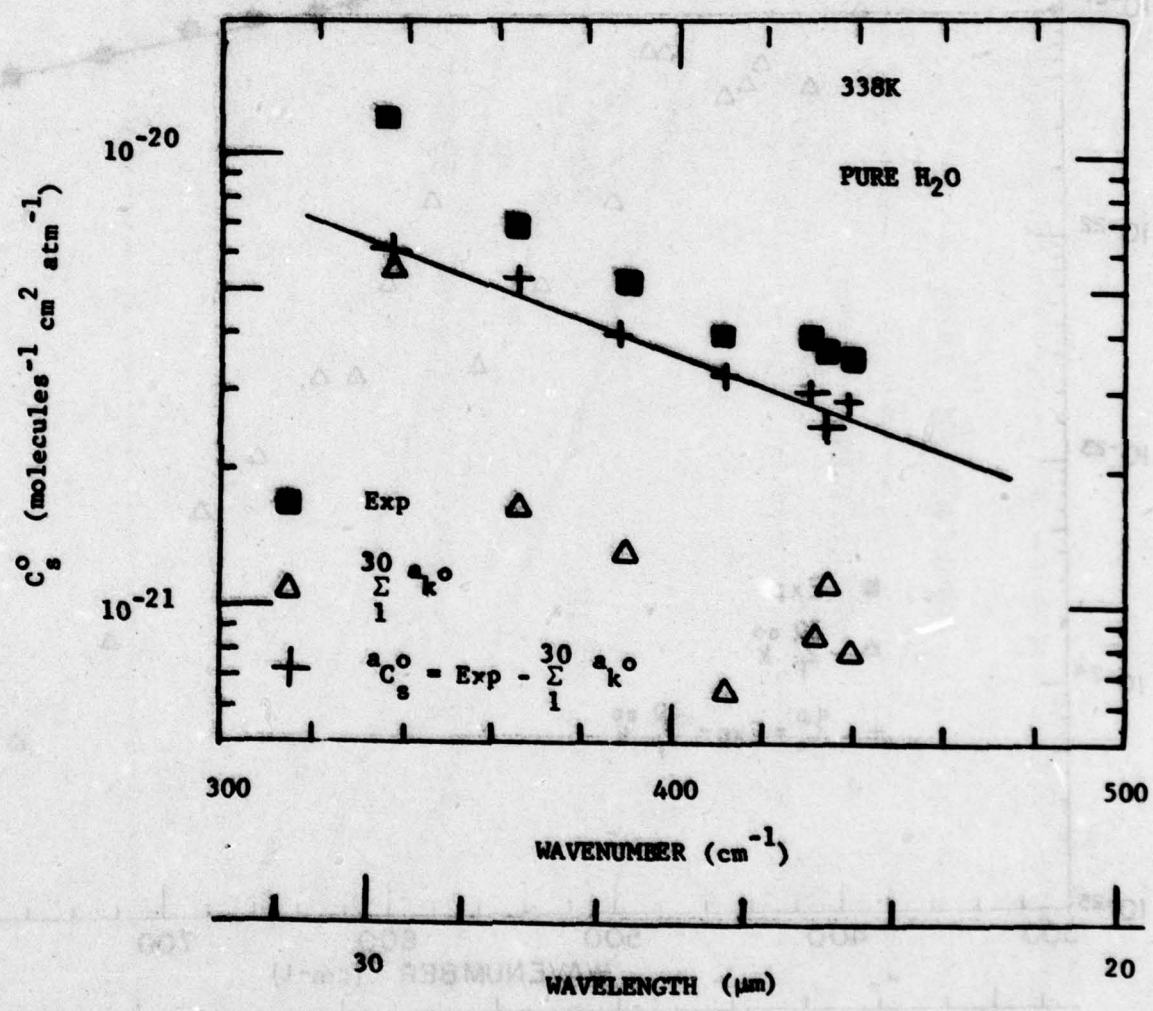


**Figure 3. Semi-logarithmic plot of the $H_2O$ continuum coefficients for self broadening at 338K**

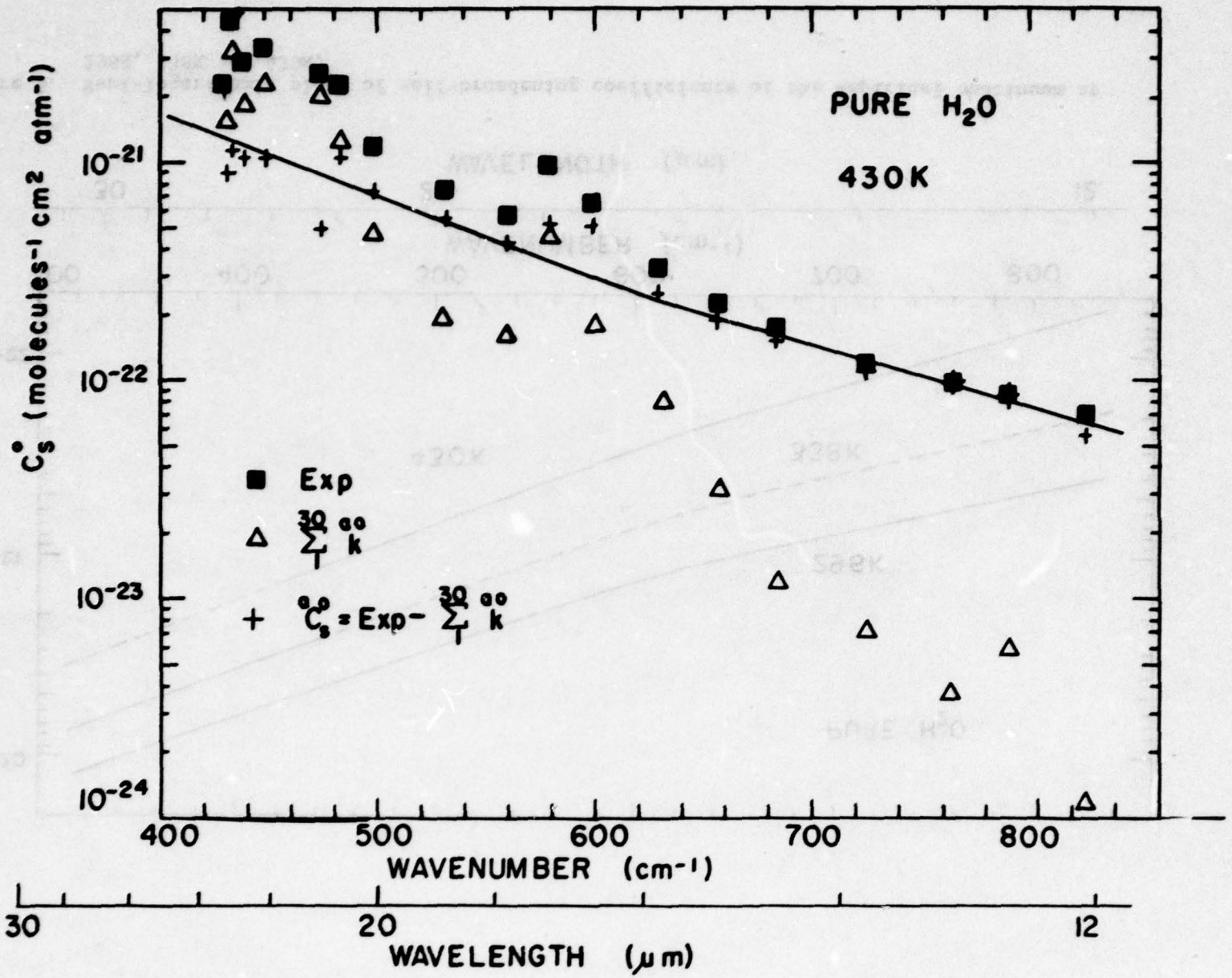


Figure 4. Semi-logarithmic plot of the $H_2O$ continuum coefficient for self broadening at 430K

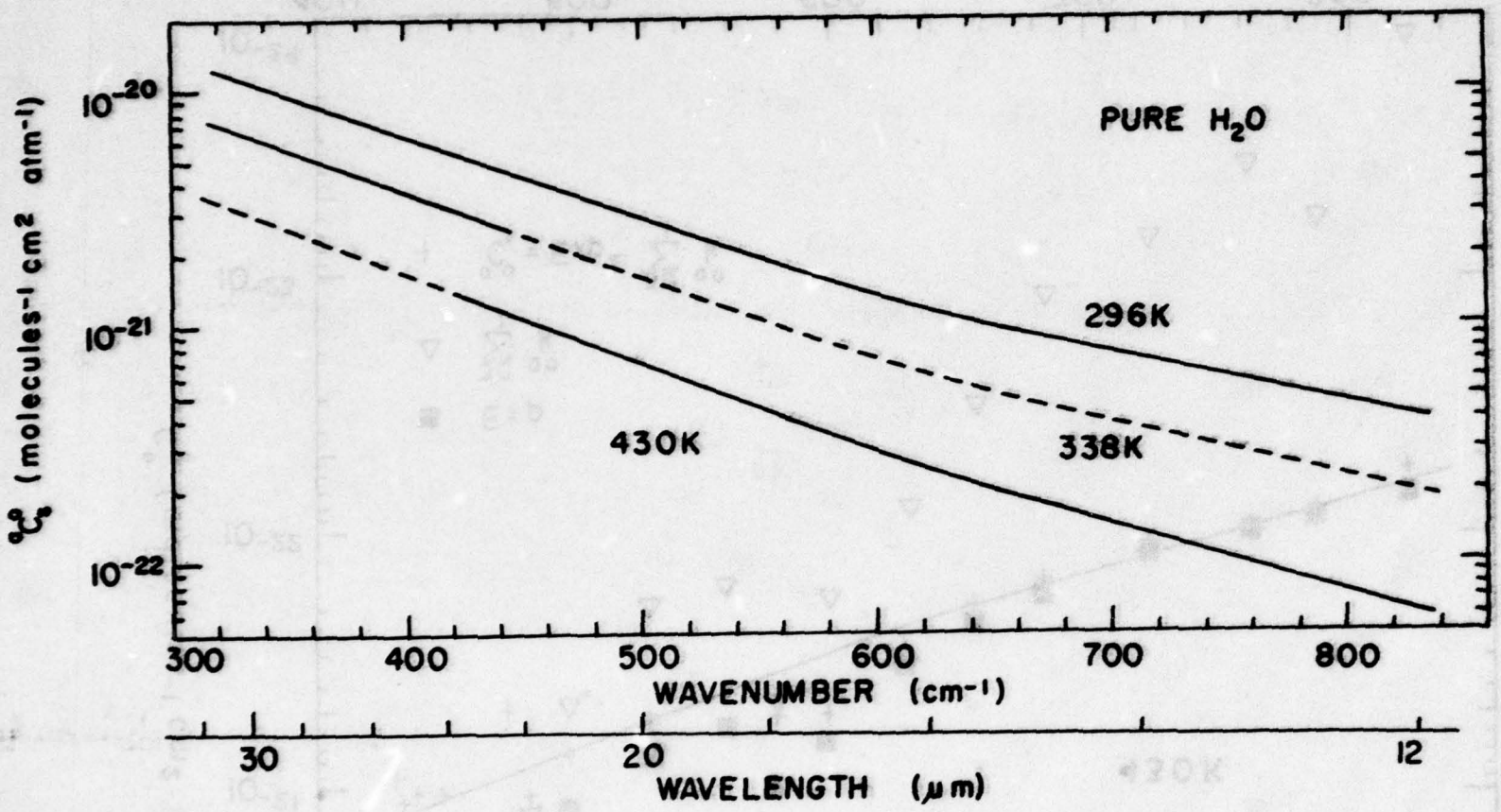


Figure 5. Semi-logarithmic plots of self-broadening coefficients of the empirical continuum at 296K, 338K and 430K.

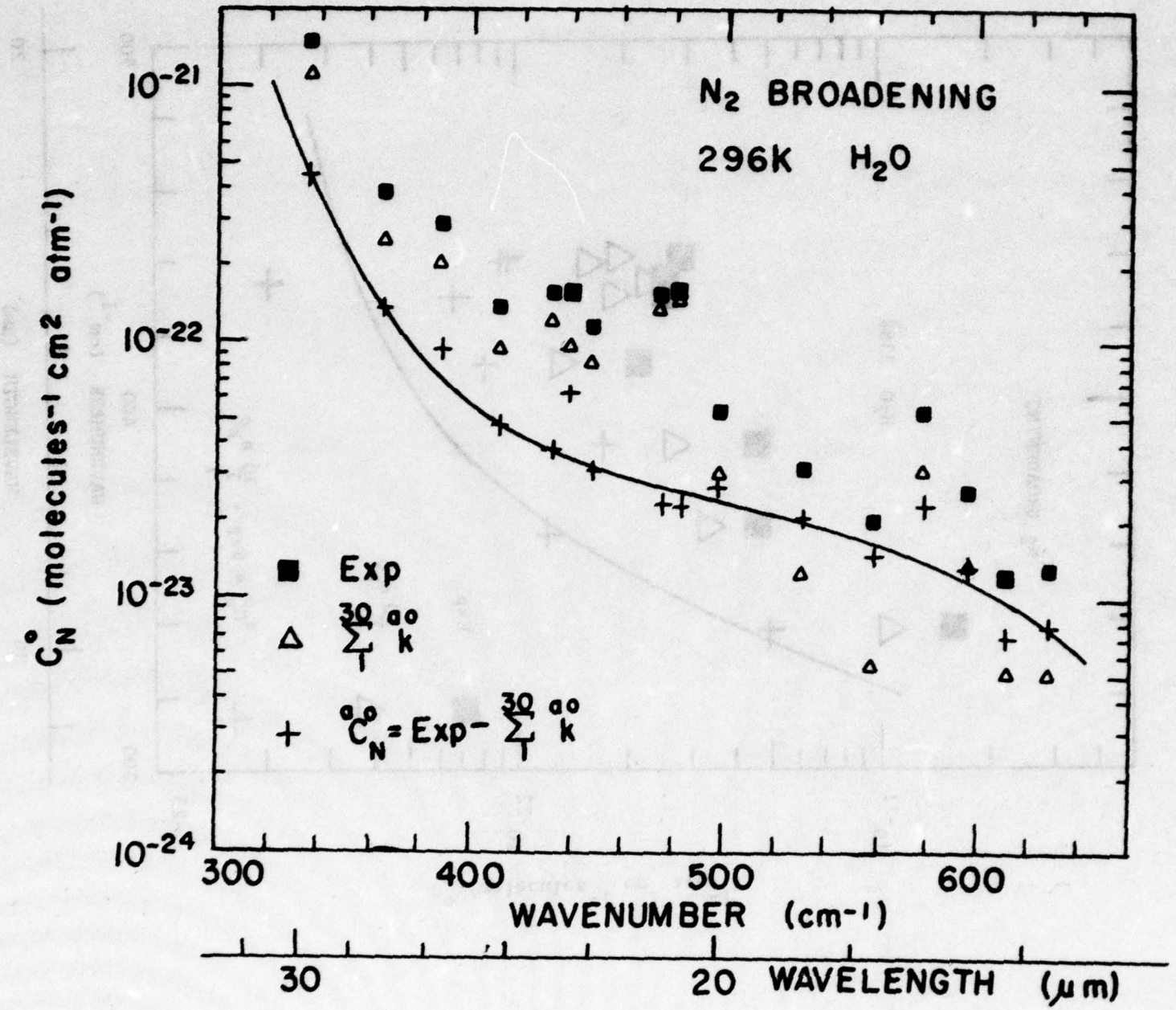


Figure 6. Semi-logarithmic plot of the $H_2O$ continuum coefficient for $N_2$ broadening at 296K.

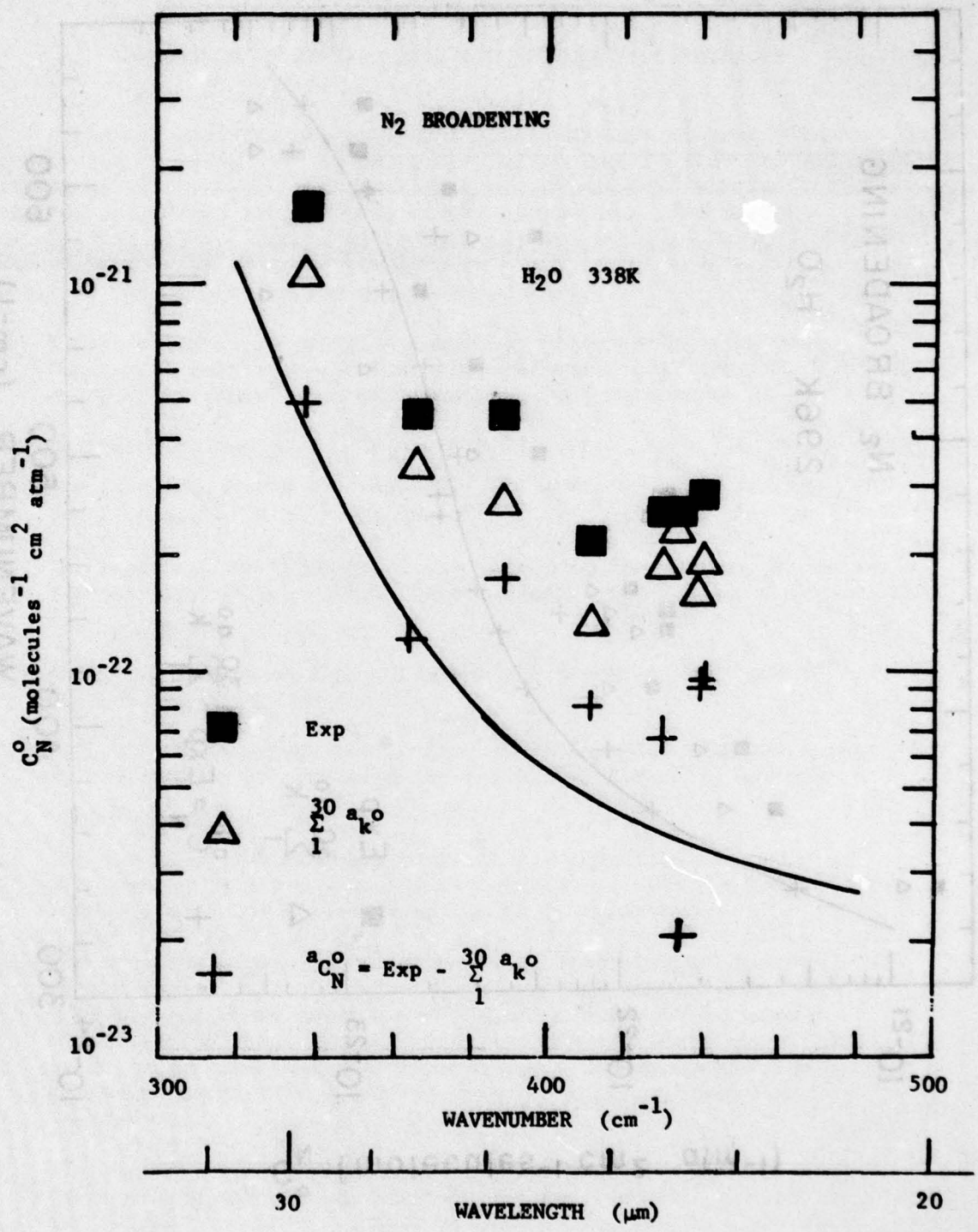


Figure 7. Semi-logarthmic plot of the $H_2O$ continuum coefficient for $N_2$ broadening at 338K.

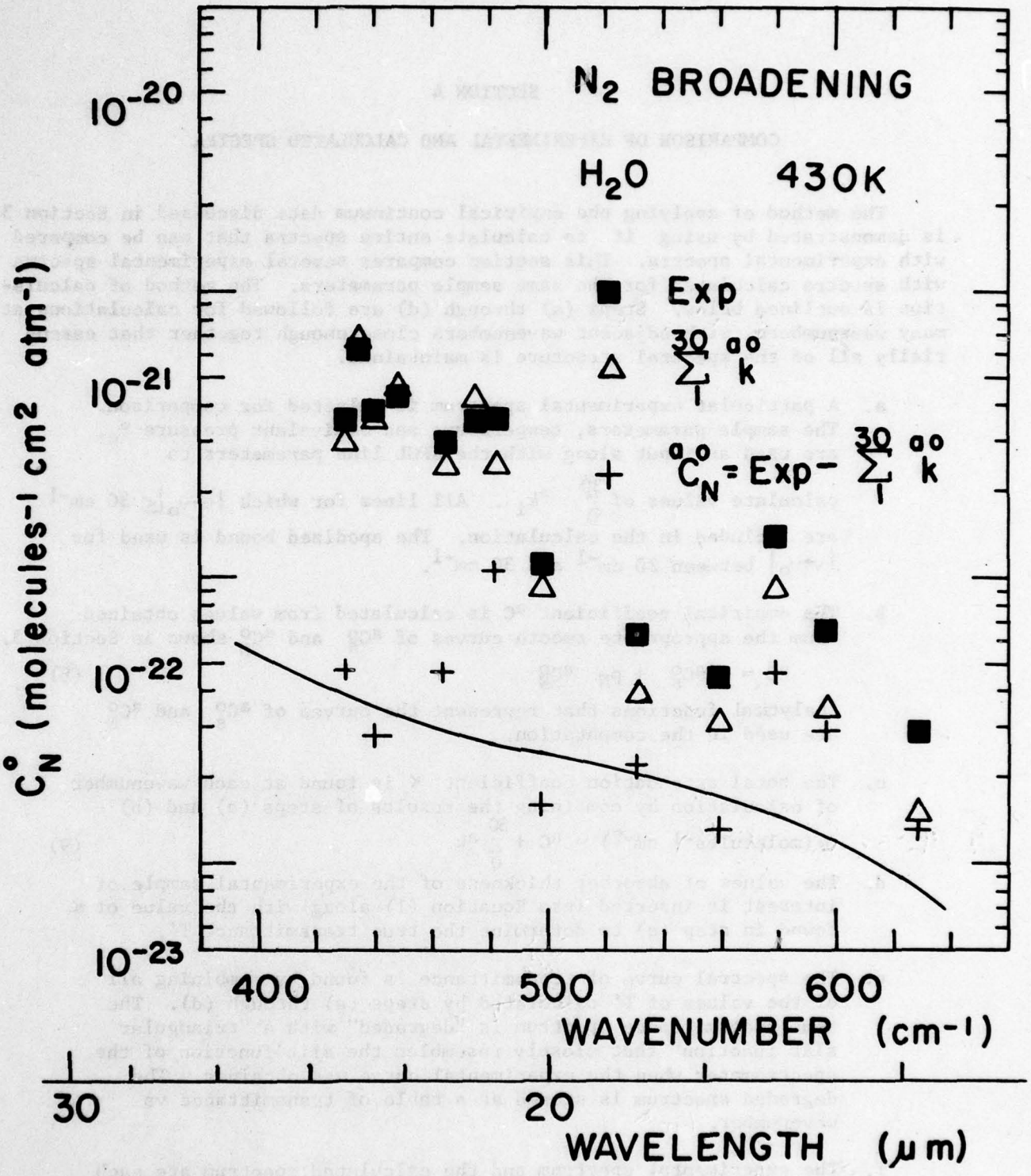


Figure 8. Semi-logarithmic plot of $H_2O$ continuum coefficient for $N_2$ broadening at 430K.

## SECTION 4

## COMPARISON OF EXPERIMENTAL AND CALCULATED SPECTRA

The method of applying the empirical continuum data discussed in Section 3 is demonstrated by using it to calculate entire spectra that can be compared with experimental spectra. This section compares several experimental spectra with spectra calculated for the same sample parameters. The method of calculation is outlined below. Steps (a) through (d) are followed for calculations at many wavenumbers, with adjacent wavenumbers close enough together that essentially all of the spectral structure is maintained.

a. A particular experimental spectrum is selected for comparison. The sample parameters, temperature and equivalent pressure $P_e$, are used as input along with the AFGL line parameters to calculate values of $\sum_{0}^{30} {}^{a}k_i$. All lines for which $|\nu-\nu_o| \leq 30$ cm$^{-1}$ are included in the calculation. The apodized bound is used for $|\nu-\nu_o|$ between 20 cm$^{-1}$ and 30 cm$^{-1}$.

b. The empirical coefficient ${}^{a}C$ is calculated from values obtained from the appropriate smooth curves of ${}^{a}C_s^o$ and ${}^{a}C_N^o$ shown in Section 3.

$$ {}^{a}C = p\ {}^{a}C_s^o + p_N\ {}^{a}C_N^o \qquad (8) $$

Analytical functions that represent the curves of ${}^{a}C_s^o$ and ${}^{a}C_N^o$ are used in the computation.

c. The total attenuation coefficient $K$ is found at each wavenumber of calculation by combining the results of steps (a) and (b)

$$ K\,(\text{molecules}^{-1}\ \text{cm}^{-2}) = {}^{a}C + \sum_{0}^{30} {}^{a}k \qquad (9) $$

d. The values of absorber thickness of the experimental sample of interest is inserted into Equation (1) along with the value of $K$ found in step (c) to determine the true transmittance T'.

e. The spectral curve of transmittance is found by combining all of the values of T' calculated by steps (a) through (d). The true transmittance spectrum is "degraded" with a "triangular slit function" that closely resembles the slit function of the spectrometer when the experimental curve was obtained. The degraded spectrum is stored as a table of transmittance vs wavenumber.

f. The experimental spectrum and the calculated spectrum are each plotted by a computer on identical scales for easy comparison. The calculated curve, represented in the figures by dots, is superimposed by hand on the experimental spectrum, which is represented by a continuous curve.

Table 2 summarizes the samples for which calculated spectra are compared with laboratory spectra. The sample numbers correspond to the ones used for the same samples in our previous reports. Columns 2-7 give the important sample parameters. Column 8 gives the spectral region covered by the spectrum, which appears in the figure designated in the last column. The resolution schedule in column 10 refers to Table 3, which gives the spectral slit width of the laboratory spectra as a function of wavenumber. While scanning a spectrum, the physical width of the spectrometer slit remains fixed, but the spectral slit-width varies because of the change in dispersion. Values of the spectral slit-width correspond approximately to the full width *at* half-maximum of a "triangular slit function". Column 9 gives the spectral slitwidth used in calculating the spectra; a constant spectral slitwidth is used over relatively wide spectral intervals.

The dots that represent the calculated spectra in Figures 9 through 21 are super-imposed on the experimental spectra with variable density so that the contour of the calculated spectra can be followed easily. A point is placed at each of the maxima and minima.

The overall agreement between the calculated and experimental spectra is seen to be quite good. Throughout large portions of many of the spectra the agreement is well within the expected experimental accuracy. The good agreement demonstrates the overall good accuracy of the AFGL line parameters and the validity of the method of using an empirical continuum to account for the contribution by the wings of distant lines. In a few places, spectral shifts by as much as 0.1 or 0.2 $cm^{-1}$ can be observed. These discrepancies are probably the result of our experimental errors; the positions of most of the line centers on the AFGL tape are undoubtedly more accurate than the wavenumber calibration of our experimental curves.

We did not adjust any of the AFGL line parameters in an attempt to improve the agreement between the experimental and calculated spectra. In only a few places is there evidence that significant improvement could be brought about by changing any of the line parameters. Some of the apparent discrepancies near very weak lines may be due to noise in the original experimental data from which the smooth curves were obtained. Errors in the experimental transmittance as large as 0.02 or 0.03 are expected in some spectral regions, particularly at low wavenumbers. Some discrepancies near line centers may be due to the difference between the experimental slitwidth and the slitwidth use in the calculations.

The relative contribution by the empirical continuum depends on the spectral region and on all of the sample parameters; temperature, absorber thickness, $H_2O$ partial pressure and $N_2$ partial pressure. Figure 15 shows spectra of two pure $H_2O$ samples for which the empirical continuum is quite important. The long, broken lines represent the transmittance that would be calculated for the empirical continuum alone. Sample 2 represented in Figure 16 consists of both $H_2O$ and $N_2$. The upper broken curve corresponds to the calculated transmittance of the empirical continuum due to self broadening only. The lower broken curve corresponds to the empirical continuum for both self broadening and $N_2$ broadening. Although $p_N$ for Sample 2 is approximately 100 times the $H_2O$ partial pressure p, the empirical continuum for $N_2$ broadening is only about the same as that for self broadening. This, of course, could be predicted from the two curves in Figures 2 and 6 that correspond to 296 .

TABLE 2

SAMPLE PARAMETERS

| Sample No | P (atm) | P (atm) | $P_e$ (atm) | L (cm) | $u^{(a)}$ (#/cm$^2$) | θ (K) | Spectral Region (cm$^{-1}$) | Resolution Schedule Calc | Exp | Figure No. |
|---|---|---|---|---|---|---|---|---|---|---|
| 182 | 0.0141 | 0.0141 | 0.0705 | 12300 | 4.30 E21 | 296 | 333-380 | 0.4 | F | 9 |
| 180 | 0.00868 | 0.00868 | 0.0434 | 12300 | 2.65 E21 | 296 | 333-380 | 0.4 | F | 9 |
| 72 | 0.0207 | 0.0207 | 0.104 | 2884 | 1.48 E21 | 296 | 333-380 | 0.4 | F | 10 |
| 81 | 0.0211 | 0.0211 | 0.106 | 420 | 2.19 E20 | 296 | 333-380 | 0.4 | F | 10 |
| 87 | 0.0105 | 0.0105 | 0.0525 | 420 | 1.10 E20 | 296 | 333-380 | 0.4 | F | 11 |
| 173 | 0.0115 | 0.0115 | 0.0575 | 59500 | 1.69 E22 | 296 | 380-443 | 0.4 | E | 12 |
| 171 | 0.00882 | 0.00882 | 0.0441 | 59500 | 1.30 E22 | 296 | 380-443 | 0.4 | E | 12 |
| 170 | 0.00553 | 0.00553 | 0.0277 | 59500 | 8.16 E21 | 296 | 380-443 | 0.4 | E | 13 |
| 61 | 0.0213 | 0.0213 | 0.107 | 2884 | 1.53 E21 | 296 | 380-443 | 0.35 | D | 13 |
| 56 | 0.0158 | 0.0158 | 0.0790 | 420 | 1.65 E20 | 296 | 380-443 | 0.35 | D | 14 |
| 3 | 0.00987 | 0.00987 | 0.0493 | 47710 | 1.17 E22 | 296 | 430-500 | 0.3 | B | 15 |
| 1 | 0.0105 | 0.0105 | 0.0527 | 12340 | 3.22 E21 | 296 | 430-500 | 0.3 | B | 15 |
| 2 | 0.00987 | 0.997 | 1.04 | 12340 | 3.02 E21 | 296 | 430-500 | 0.3 | B | 16 |
| 4 | 0.0199 | 0.0199 | 0.0993 | 35920 | 1.76 E22 | 296 | 495-633 | 0.35 | A | 17 |
| 5 | 0.0121 | 1.04 | 1.05 | 47710 | 1.43 E22 | 296 | 495-633 | 0.35 | A | 18 |
| 111 | 0.0326 | 0.0326 | 0.163 | 2884 | 2.08 E21 | 333 | 333-380 | 0.4 | F | 19 |
| 104 | 0.0213 | 0.0213 | 0.107 | 420 | 1.95 E20 | 338 | 333-380 | 0.4 | F | 19 |
| 115 | 0.0208 | 0.0208 | 0.104 | 2884 | 1.30 E21 | 338 | 380-442 | 0.35 | D | 14 |
| 45 | 0.0685 | 0.0685 | 0.343 | 416 | 4.92 E20 | 424 | 440-500 | 0.4 | C | 20 |
| 43 | 0.0198 | 0.0198 | 0.0990 | 416 | 1.42 E20 | 424 | 440-500 | 0.4 | C | 20 |
| 41 | 0.100 | 0.100 | 0.500 | 416 | 7.14 E20 | 428 | 495-633 | 0.6 | C | 21 |

(a) The unit molecules/cm$^2$ is abbreviated #/cm$^2$

TABLE 3

SPECTRAL RESOLUTION SCHEDULE

| $\nu$ ($cm^{-1}$) | A ($cm^{-1}$) | B ($cm^{-1}$) | C ($cm^{-1}$) | D ($cm^{-1}$) | E ($cm^{-1}$) | F ($cm^{-1}$) |
|---|---|---|---|---|---|---|
| 330 | | | | | | 0.28 |
| 340 | | | | | | 0.31 |
| 350 | | | | | | 0.33 |
| 360 | | | | | | 0.36 |
| 370 | | | | | | 0.39 |
| 380 | | | | 0.23 | 0.32 | 0.42 |
| 390 | | | | 0.25 | 0.34 | 0.46 |
| 400 | | | | 0.28 | 0.36 | |
| 410 | | | | 0.30 | 0.39 | |
| 420 | | | | 0.32 | 0.42 | |
| 430 | | 0.26 | | 0.35 | 0.45 | |
| 440 | | 0.27 | 0.35 | 0.37 | 0.48 | |
| 450 | | 0.28 | 0.37 | 0.39 | 0.51 | |
| 460 | | 0.29 | 0.39 | | | |
| 470 | | 0.31 | 0.41 | | | |
| 480 | | 0.33 | 0.43 | | | |
| 490 | | 0.34 | 0.45 | | | |
| 500 | 0.26 | 0.35 | 0.46 | | | |
| 510 | 0.28 | | 0.48 | | | |
| 520 | 0.29 | | 0.50 | | | |
| 530 | 0.31 | | 0.53 | | | |
| 540 | 0.33 | | 0.55 | | | |
| 550 | 0.35 | | 0.57 | | | |
| 560 | 0.36 | | 0.59 | | | |
| 570 | 0.38 | | 0.61 | | | |
| 580 | 0.40 | | 0.63 | | | |
| 590 | 0.42 | | 0.65 | | | |
| 600 | 0.43 | | 0.67 | | | |
| 610 | 0.45 | | 0.69 | | | |
| 620 | 0.47 | | 0.71 | | | |
| 630 | 0.49 | | 0.73 | | | |

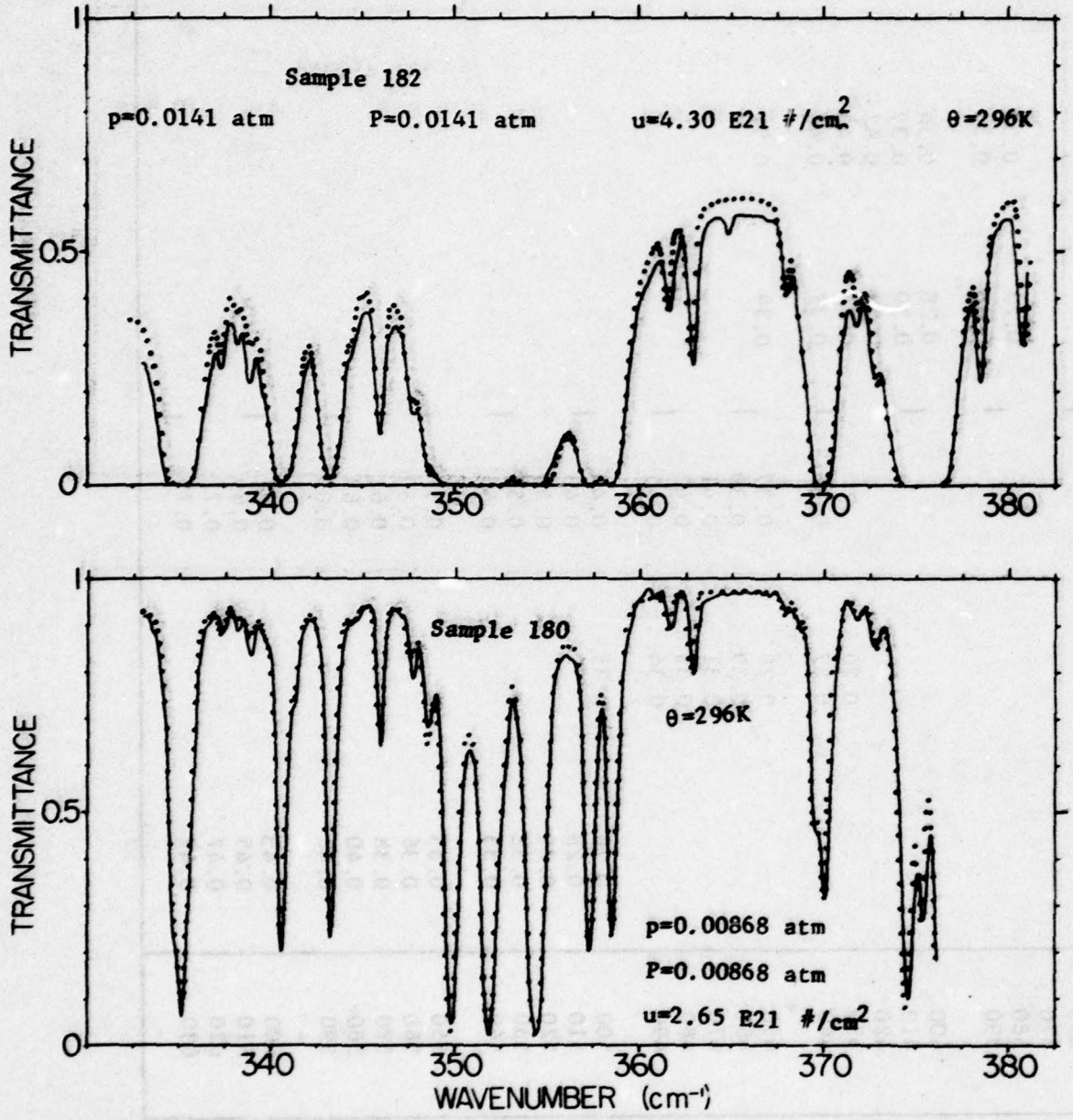


Figure 9. Comparison of experimental and calculated spectra from 333 to 380 $cm^{-1}$ for 2 samples of $H_2O$ at 296K.

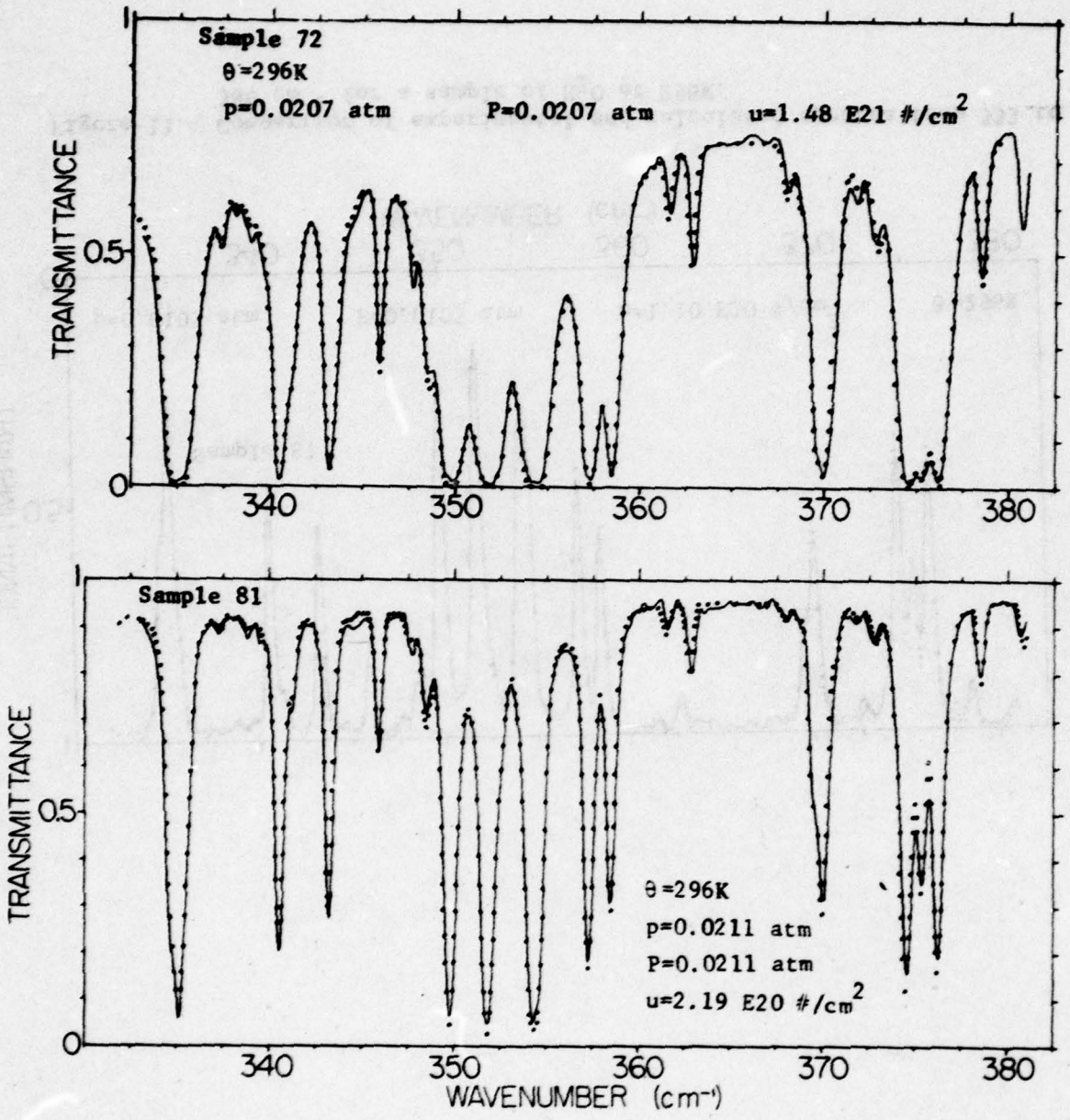


Figure 10. Comparison of experimental and calculated spectra from 333 to 380 $cm^{-1}$ for 2 samples of $H_2O$ at 296K.

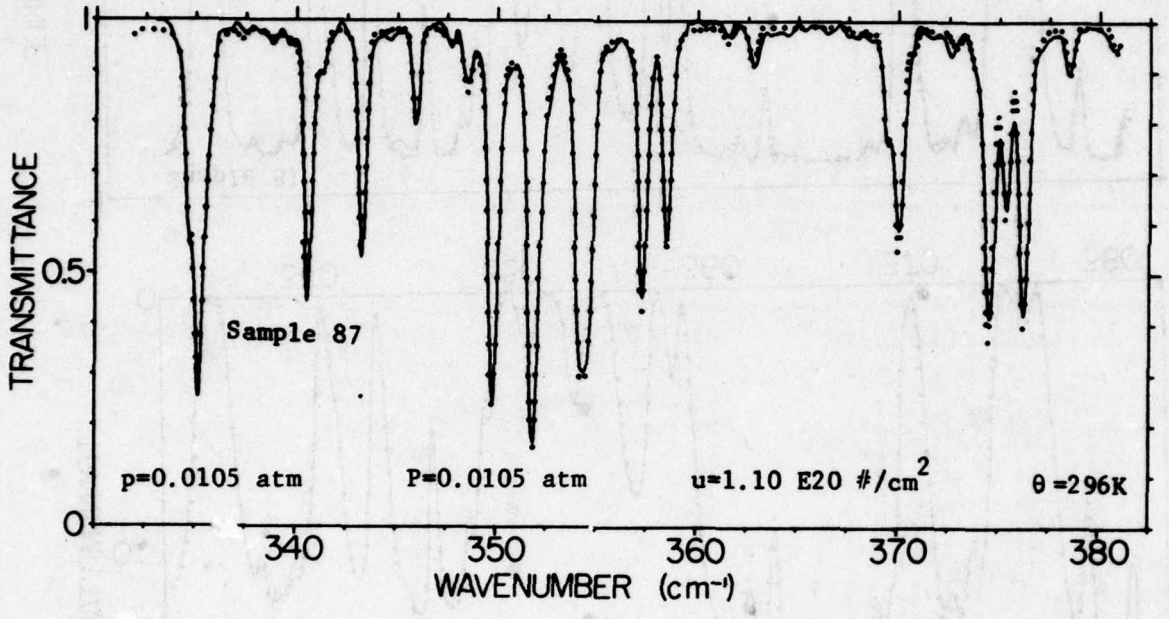


**Figure 11. Comparison of experimental and calculated spectra from 333 to 380 $cm^{-1}$ for a sample of $H_2O$ at 296K.**

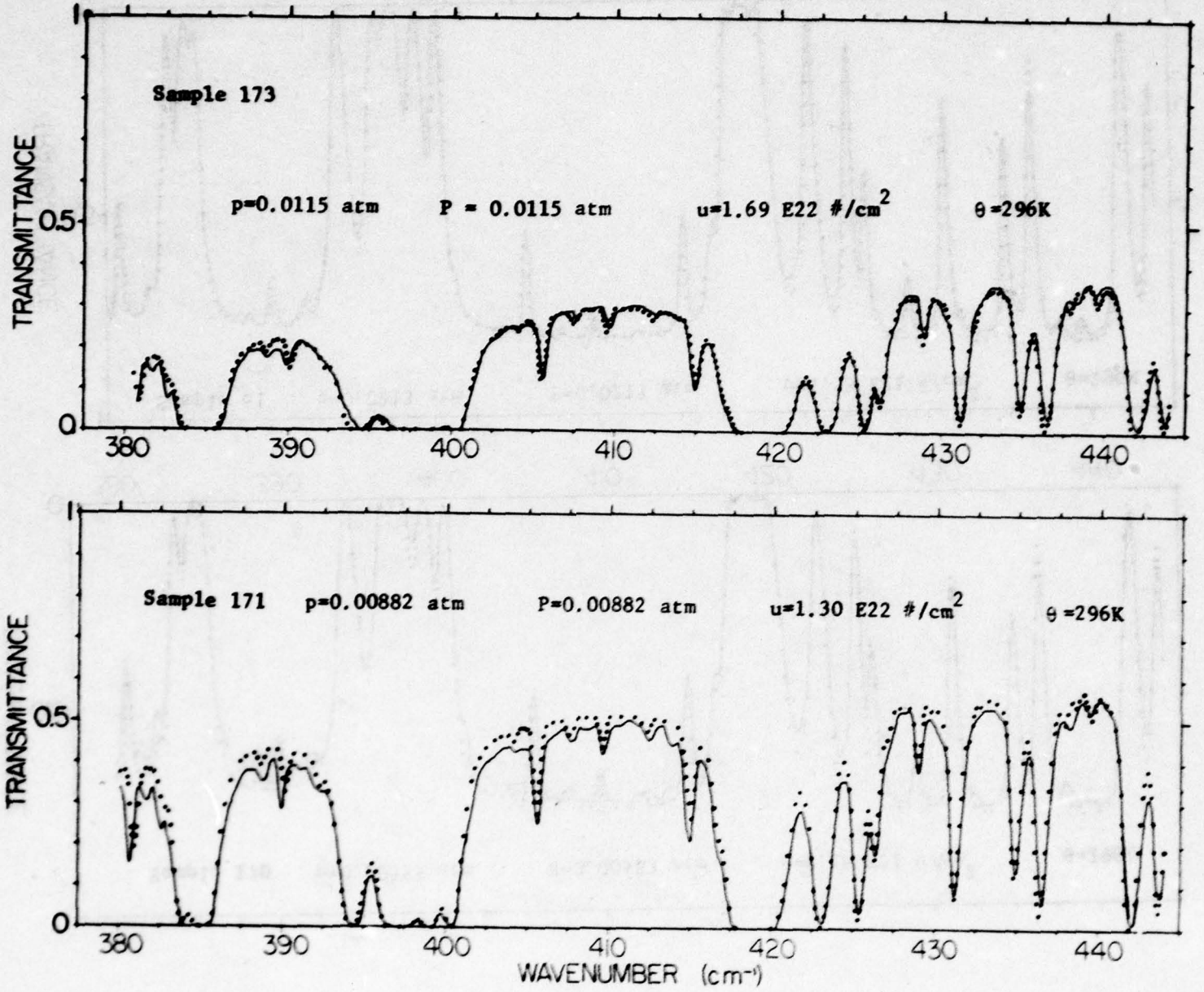


Figure 12. Comparison of experimental and calculated spectra from 380 to 443 $cm^{-1}$ for 2 samples of $H_2O$ at 296K.

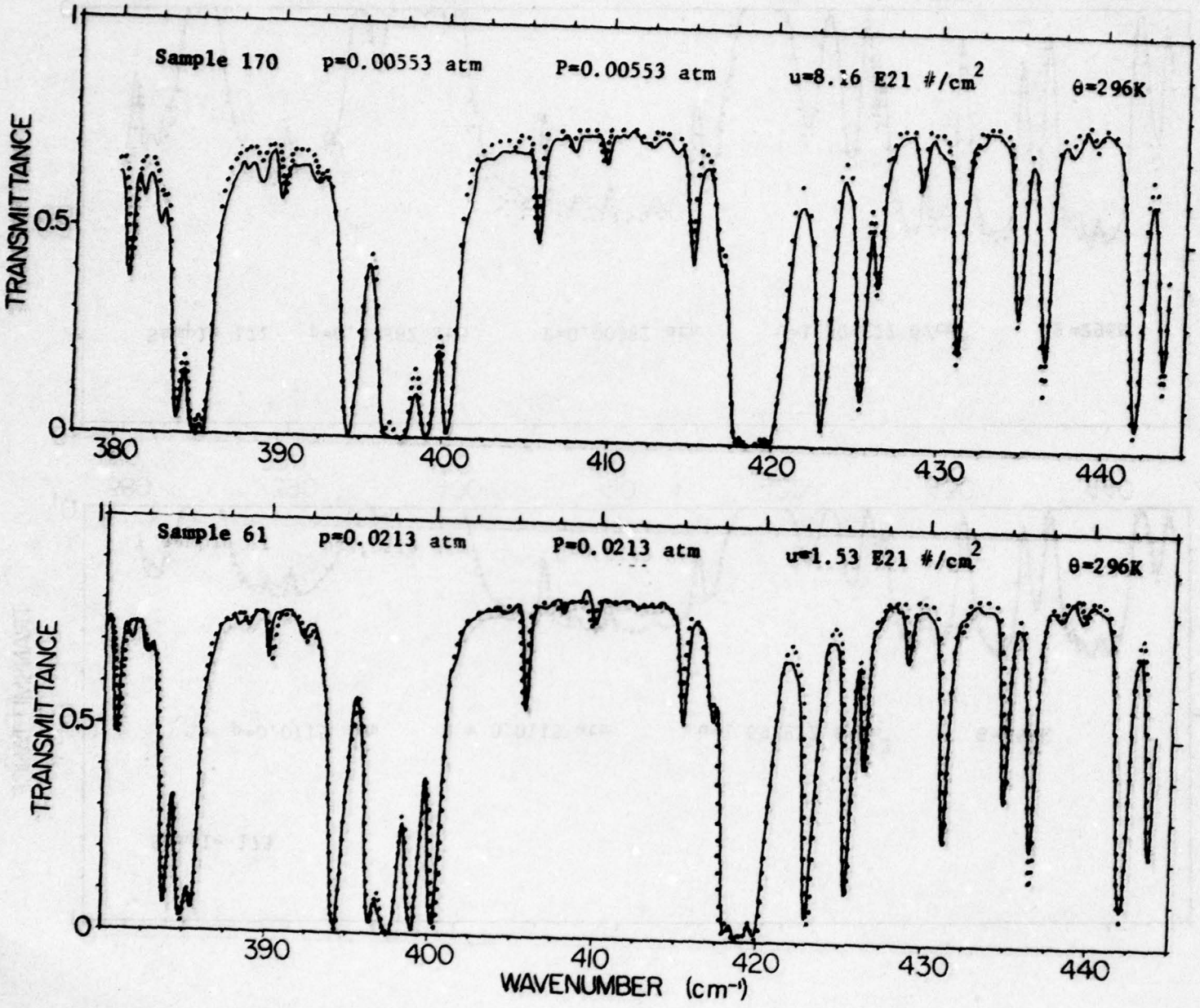


Figure 13. Comparison of experimental and calculated spectra from 380 to 443 $cm^{-1}$ for 2 samples of $H_2O$ at 296K.

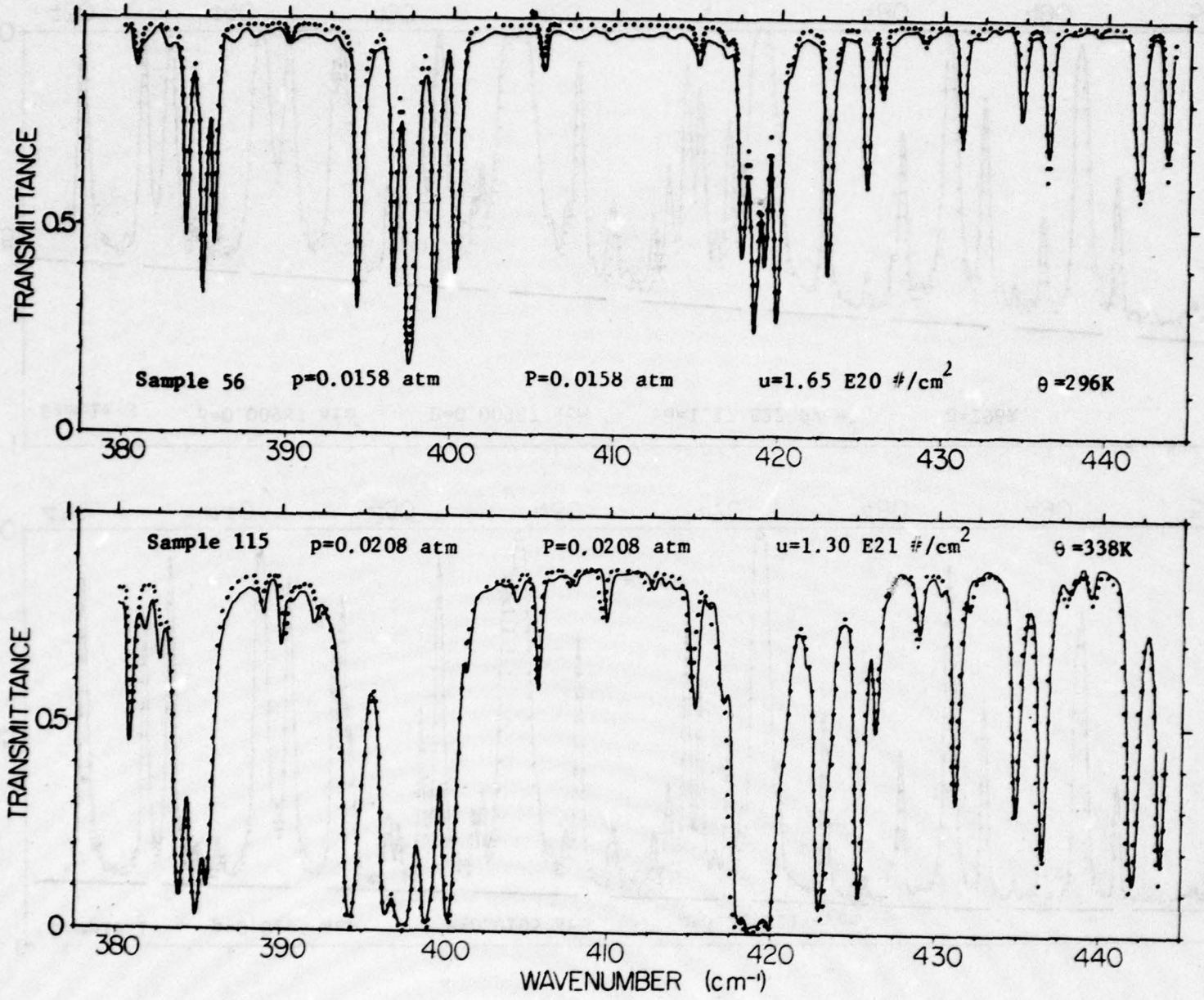


Figure 14. Comparison of experimental and calculated spectra from 380 to 443 $cm^{-1}$ for 2 samples of $H_2O$.

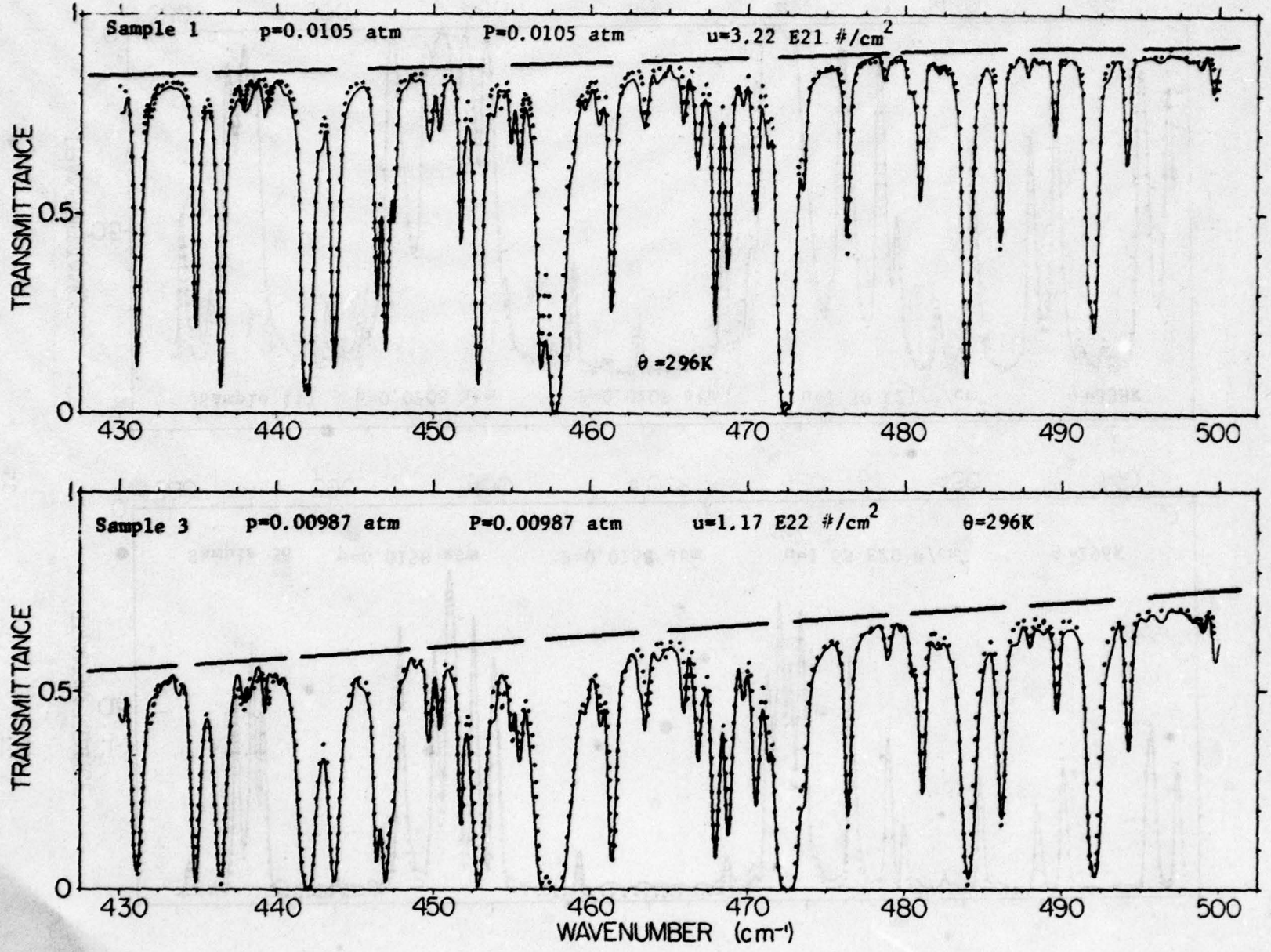


Figure 15. Comparison of experimental and calculated spectra from 430 to 500 $cm^{-1}$ for 2 samples of $H_2O$ at 296K.

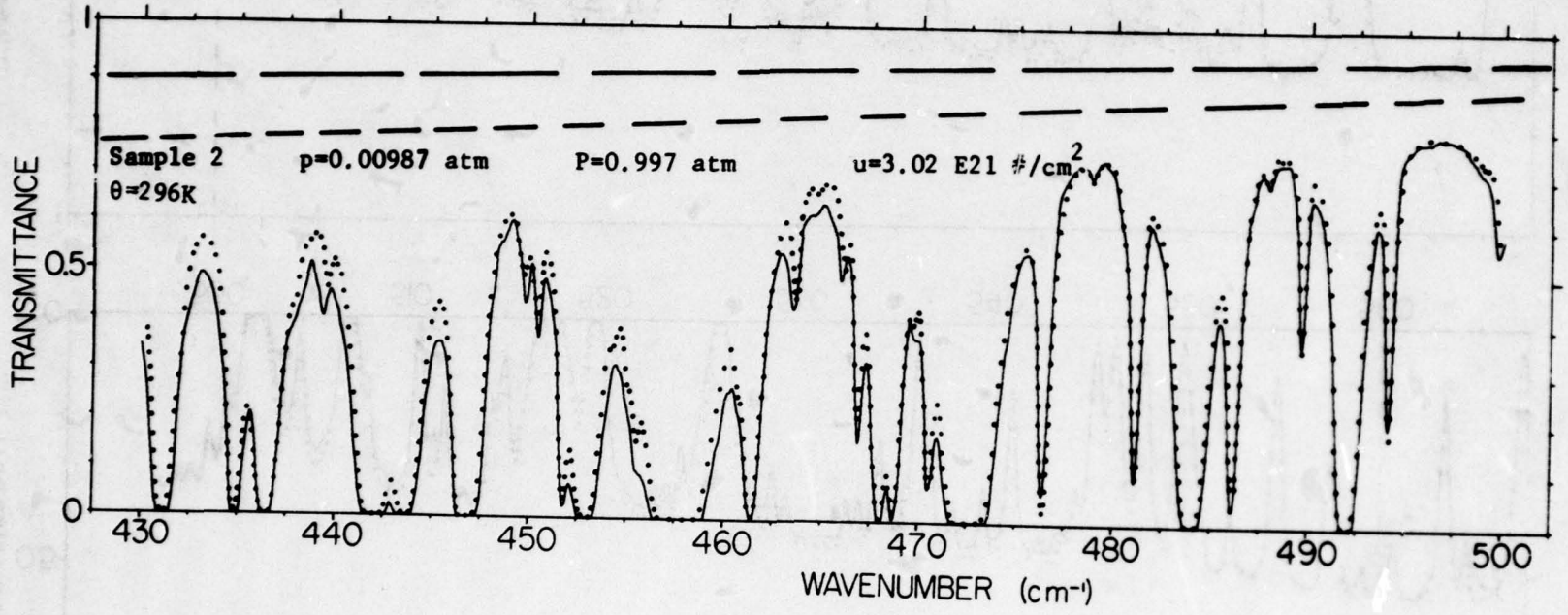


Figure 16. Comparison of experimental and calculated spectra from 430 to 500 $cm^{-1}$ for a sample of $H_2O$ at 296K.

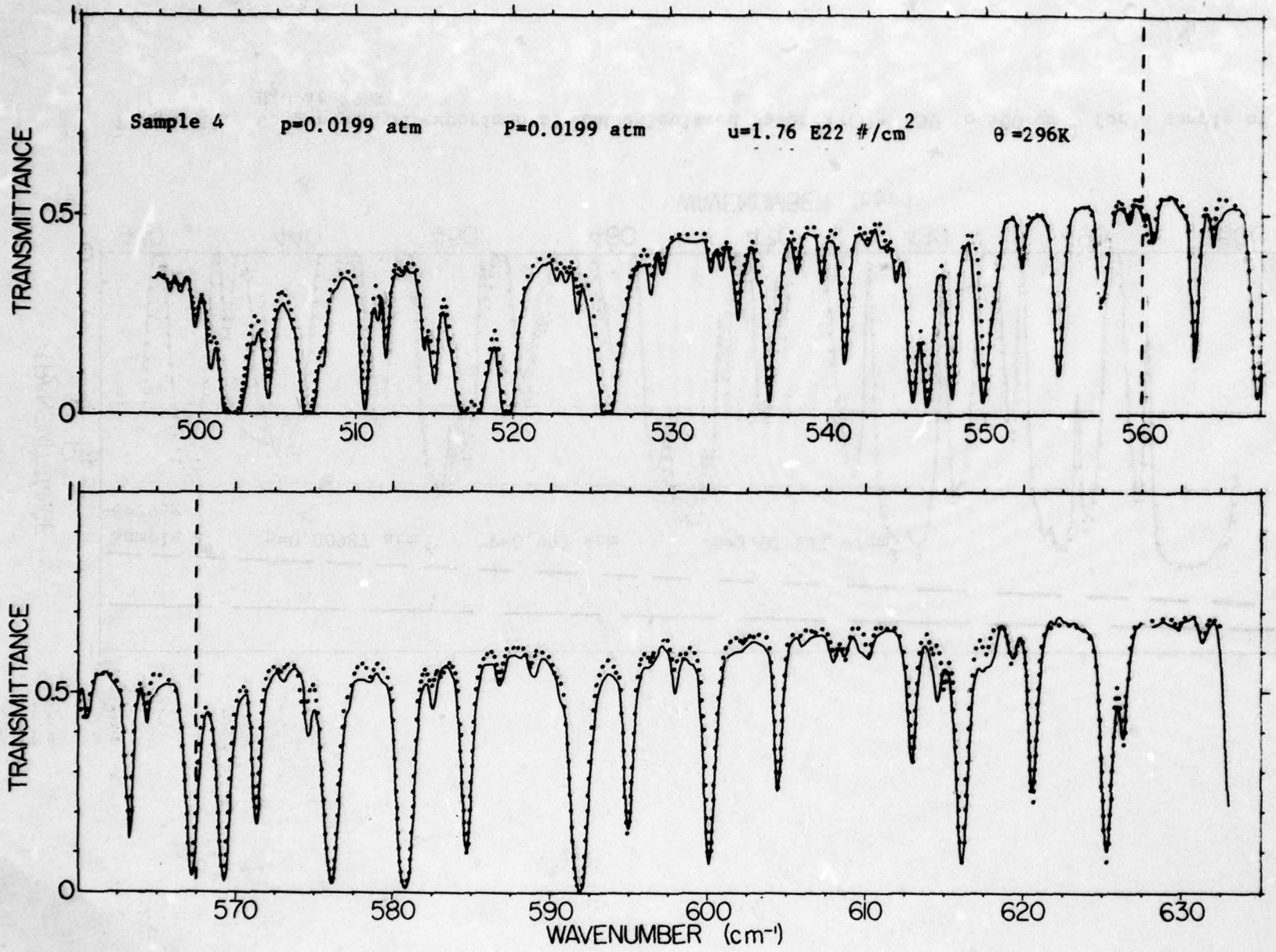


Figure 17. Comparison of experimental and calculated spectra from 495 to 633 $cm^{-1}$ for a sample of $H_2O$ at 296K.

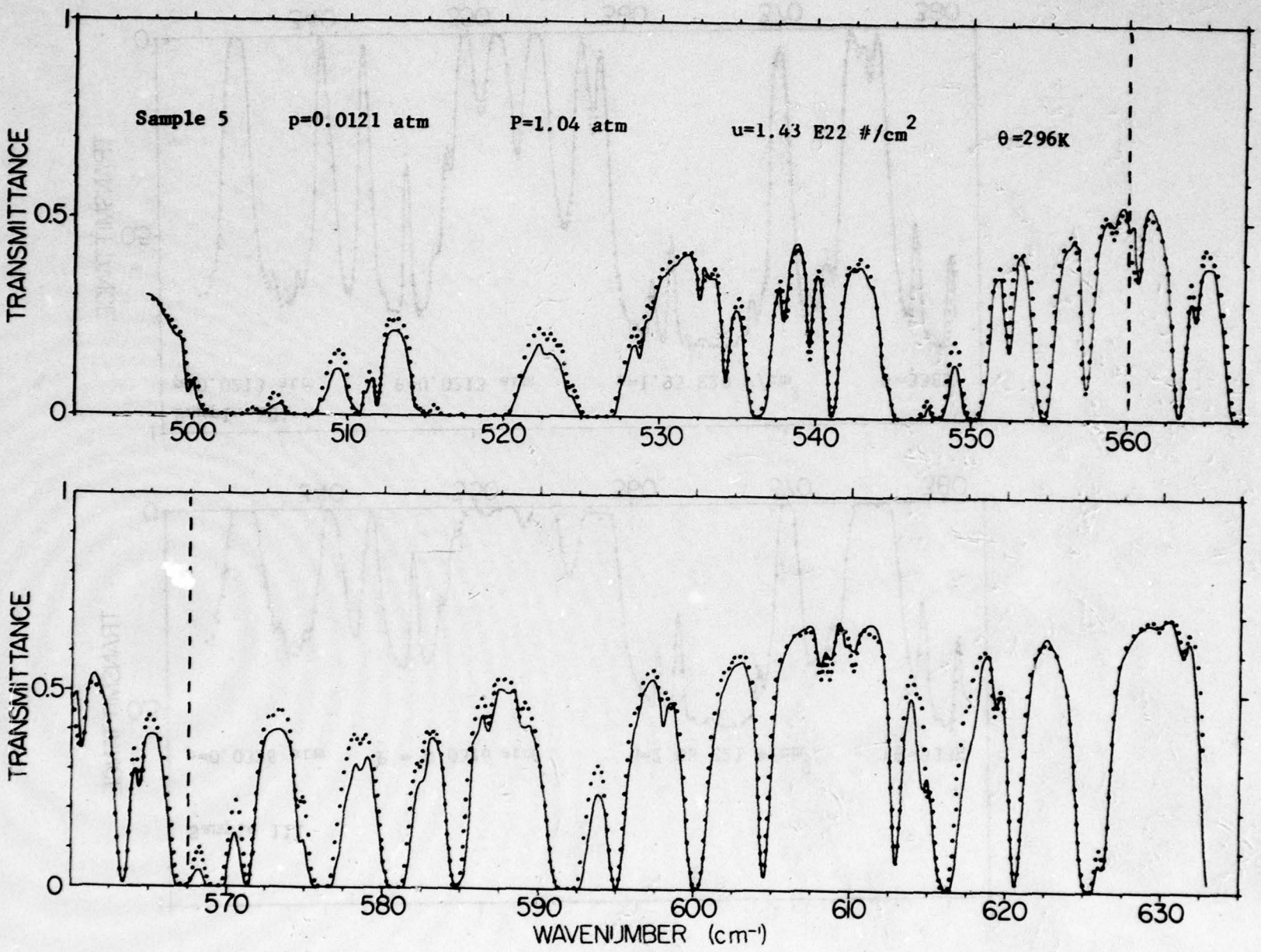


Figure 18. Comparison of experimental and calculated spectra from 495 to 633 $cm^{-1}$ for a sample of $H_2O$ at 296K.

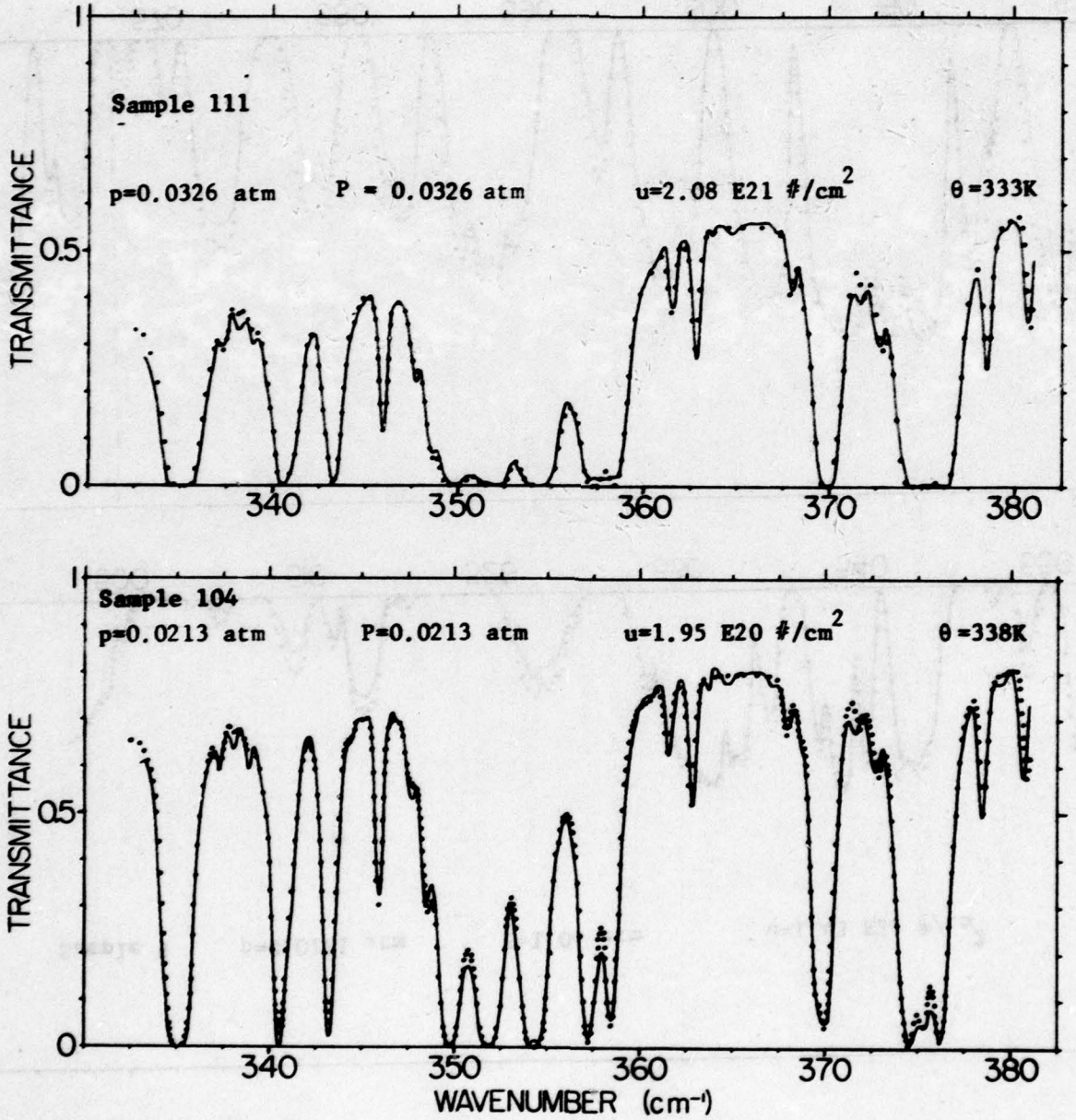


Figure 19. Comparison of experimental and calculated spectra from 333 to 380 $cm^{-1}$ for 2 samples of $H_2O$ at 333K.

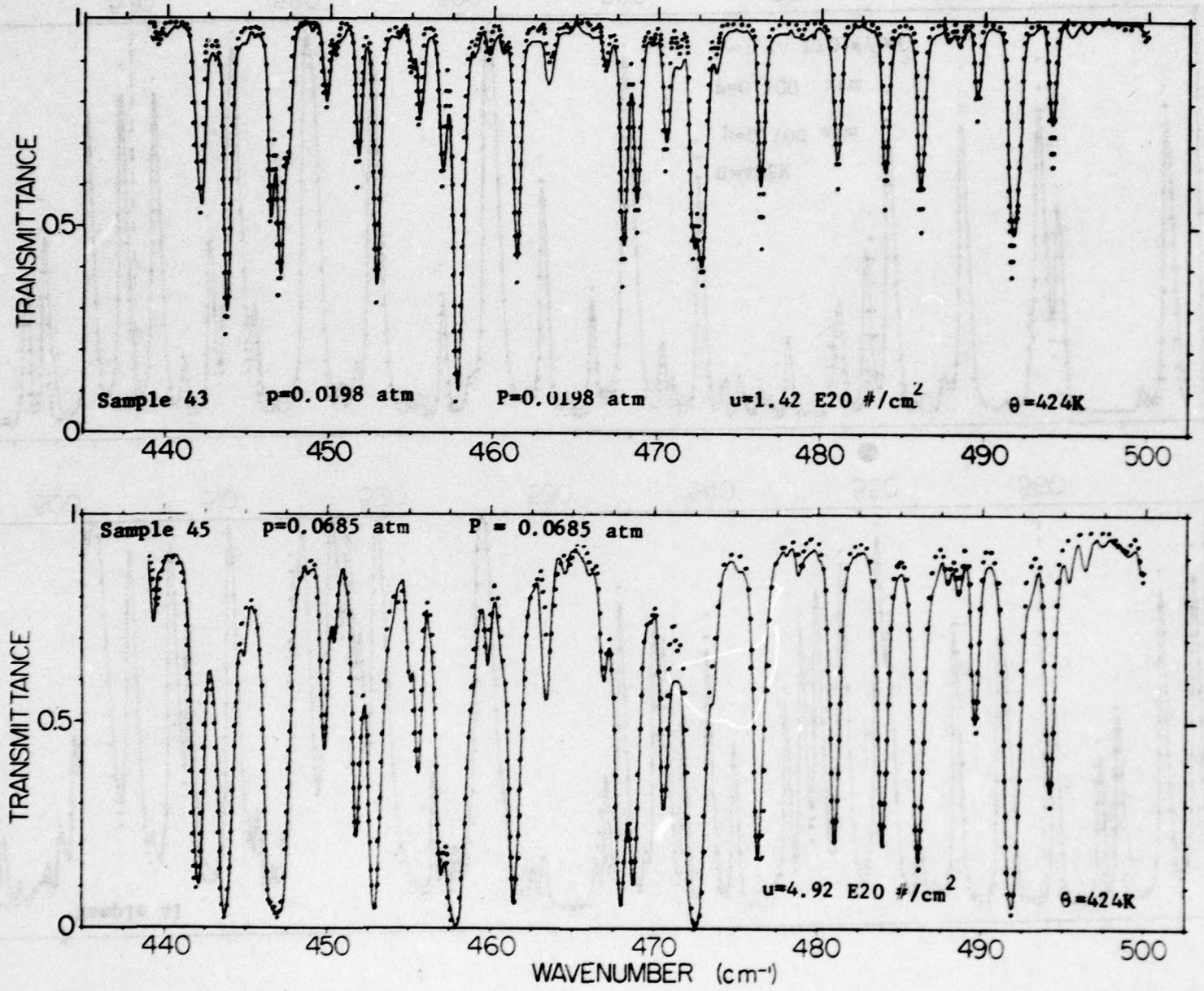


Figure 20. Comparison of experimental and calculated spectra from 440 to 500 $cm^{-1}$ for 2 samples of $H_2O$ at 424K.

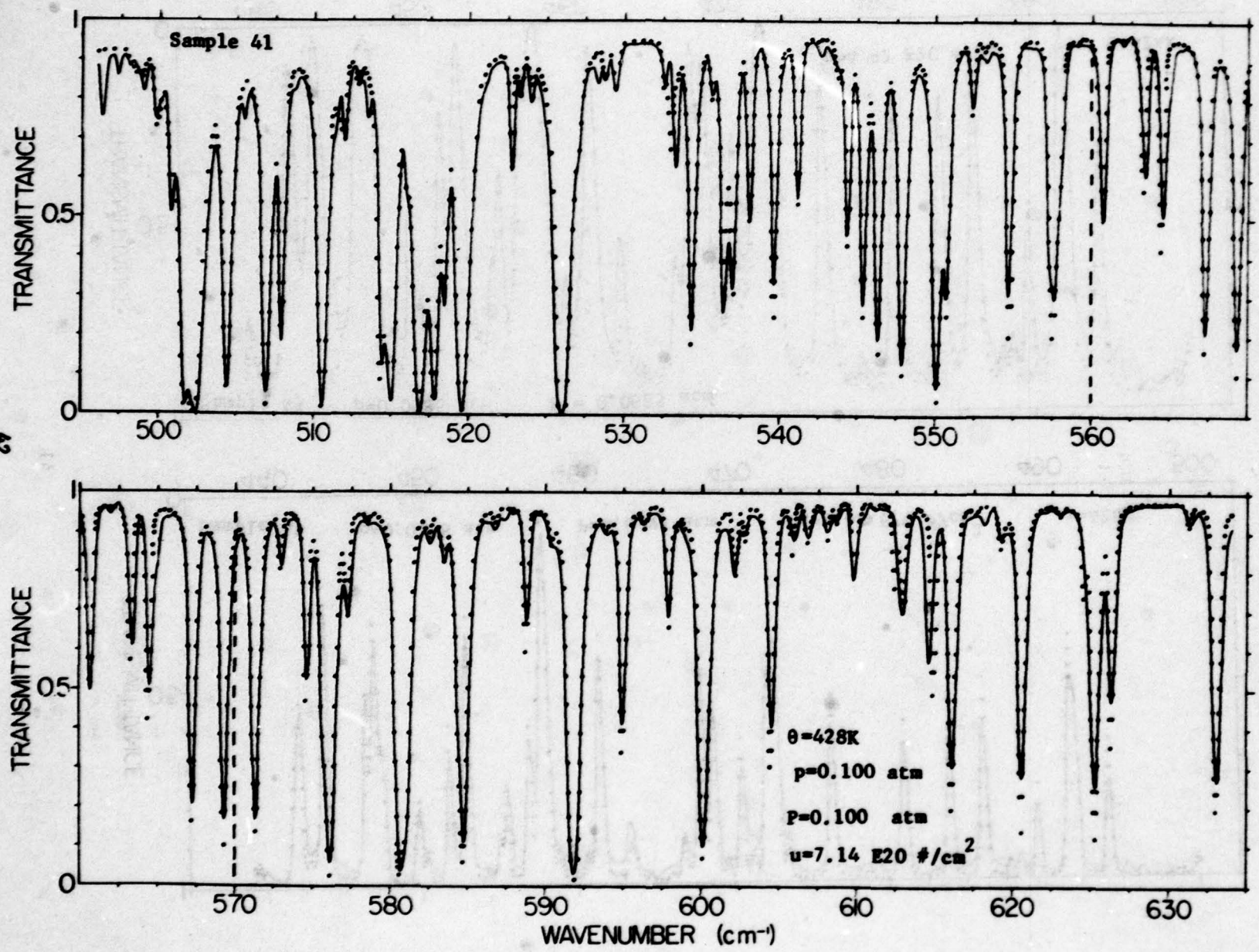


Figure 21. Comparison of experimental and calculated spectra from 495 to 633 $cm^{-1}$ for a sample of $H_2O$ at 428K.

## SECTION 5

## APPLICATION TO CALCULATIONS OF ATMOSPHERIC TRANSMITTANCE

It was demonstrated in Section 4 that spectral curves of transmittance can be calculated quite accurately by using the empirical continuum in conjunction with the AFGL line parameters. The calculated spectra correspond to samples at the same temperatures at which the empirical continuum was determined. For atmospheric applications, it is essential that the empirical continuum can be calculated for a wide variety of temperatures and pressures. The pressure dependence is quite predictable, but it is necessary to extrapolate the continuum coefficients to temperatures well below those at which we obtained experimental data.

In previous work[13] we have found that the continuum attenuation coefficient at a given wavenumber can usually be fitted to an equation of the form:

$$ {}^{a}C^{o} \text{ (at } \theta) = {}^{a}C^{o} \text{ (at } \theta^{o}) \exp\left[\frac{b}{\theta} - \frac{b}{\theta^{o}}\right] \qquad (10) $$

We have found that this equation can also be used to fit the empirical continuum for self broadening in the spectral regions where we obtained data at three or more temperatures. The reference temperature, $\theta^{o}$, in our calculations is 296K. Data for three temperatures (296K, 338K and 430K) are shown in Figures 2, 3 and 4 near 430 $cm^{-1}$. Data presented previously by us[3] on continuum absorption at 358 K and 388K between 700 $cm^{-1}$ and 800 $cm^{-1}$ have also been used in conjunction with the 296K and 430K data from Section 3 to determine values of the coefficient b for several wavenumbers. At each of these wavenumbers, the data fitted, within the experimental uncertainty, a curve based on Equation (10) with the appropriate value of b. This good agreement for 3 temperatures provides some evidence of the validity of an equation of this form. Of course, it should not be assumed that the equations are completely valid for temperatures well outside the range covered by the experimental data.

Because of the apparent validity of Equation (10) in spectral regions where it could be checked, we have assumed that it is valid for the entire spectral region and temperatures covered in this report. Accordingly, we have used the data presented in Section 3 to determine the appropriate values of the coefficient b. The results are summarized in Table 4.

We have used the values of b shown in Table 4 to calculate ${}^{a}C_{s}^{o}$ at several different temperatures that represent any part of the earth's atmosphere where a significant amount of $H_2O$ vapor exists. In addition to the values of ${}^{a}C_{s}^{o}$ calculated at 10K intervals, Table 5 includes the values for the three temperatures (296K, 338K and 430K) at which the experimental data exist. Because of the exponential form of Equation (10), the values of ${}^{a}C_{s}^{o}$ calculated for the very low temperatures are much greater than the corresponding values at room temperature (296K). The large temperature range over which the

13. Darrell E. Burch, David A. Gryvnak, and John D. Pembrook, Investigation of the Absorption by Atmospheric Gases:Water, Nitrogen, Nitrous Oxide Semi-Annual Technical Report No. ° AFCRL-71-0124. Aeronutronic Report No. U-4897, January, 1971.

extrapolation results in a relatively high uncertainty for the values calculated for temperatures below approximately 250K. The seriousness of this uncertainty in calculating atmospheric transmittance, however, is partially offset by the very low partial pressures of $H_2O$ vapor that exist at low temperatures.

The results given in Section 3 indicate that the ratio $^{a}C^{o}/\sum_{1}^{30} {}^{a}k^{o}$ is much less for $N_2$ broadening than for self broadening. This ratio also decreases with increasing temperature. Because of the relatively small contribution by the empirical continuum, the coefficients can not be determined as accurately for $N_2$ broadening as for self broadening. Table 6 lists values of $^{a}C^{o}_{N}$ from the curve of Figure 6 for 296K. As pointed out in Section 3, the smallness of $^{a}C^{o}_{N}$ and the relatively poor accuracy with which this quantity could be measured made it impractical to determined its temperature dependence. Therefore, we recommend that the values determined for $^{a}C^{o}_{N}$ at 296K be used for all calculations involving the earth's atmosphere.

The rapid decrease in the attenuation by the empirical continuum at reduced temperature is illustrated in Table 7. The second column of this table gives values of the attentuation coefficient $\beta_L$ (in $km^{-1}$) calculated from the values of $^{a}C^{o}_{s}$ and $^{a}C^{o}_{N}$ presented in Section 3 for the empirical continuum in an atmosphere saturated with $H_2O$ vapor at 296K. (The $H_2O$ density is actually based on 23°C, which is 296.3K) At this temperature the vapor pressure of $H_2O$ is approximately 0.0277 atm and the value of u for a 1-kilometer path is 6.89 E20 molecules/$cm^2$. Values of $^{a}C^{o}_{N}$ and $^{a}C^{o}_{s}$ calculated for 240K by use of Equation (10) have served as the basis for the coefficients given in the third column for saturated air at 240K and 1 atm total pressure. The final column illustrates the influence of reduced total pressure. These data represent saturated air at 240K at the total pressure that corresponds to this temperature in the midlatitude Summer Model Atmosphere [14]. At this low temperature, very long atmospheric paths are required for the empirical continuum absorption to be significant. The contribution is even less at temperatures below 240K because of the decreased vapor pressure of $H_2O$. It is emphasized that the coefficients in Table 7 represent only the empirical continuum. The total attenuation coefficient is calculated by adding the empirical continuum coefficient to the calculated sum $\sum_{1}^{30} a_k$, of the contributions of the lines.

---

14. R. A. McClatchey, R. W. Fenn, J. E. A. Selby, F. E. Volz, and J. S. Garing, "Optical Properties of the Atmosphere" (Third Edition) Report No. AFCRL-72-0497, Environmental Research Papers, No. 41. August 1972.

TABLE 4

TEMPERATURE COEFFICIENT FOR THE EMPIRICAL $H_2O$ CONTINUUM

| $\nu$ ($cm^{-1}$) | b (K) | $\nu$ ($cm^{-1}$) | b (K) |
|---|---|---|---|
| 320. | 1197 | | |
| 330. | 1206 | | |
| 340. | 1214 | | |
| 350. | 1223 | 600. | 1442 |
| 360. | 1231 | 610. | 1454 |
| 370. | 1240 | 620. | 1467 |
| 380. | 1248 | 630. | 1481 |
| 390. | 1257 | 640. | 1495 |
| 400. | 1265 | 650. | 1510 |
| 410. | 1273 | 660. | 1525 |
| 420. | 1282 | 670. | 1542 |
| 430. | 1290 | 680. | 1560 |
| 440. | 1299 | 690. | 1579 |
| 450. | 1307 | 700. | 1597 |
| 460. | 1316 | 710. | 1615 |
| 470. | 1324 | 720. | 1633 |
| 480. | 1333 | 730. | 1652 |
| 490. | 1341 | 740. | 1670 |
| 500. | 1349 | 750. | 1688 |
| 510. | 1358 | 760. | 1706 |
| 520. | 1366 | 770. | 1725 |
| 530. | 1375 | 780. | 1743 |
| 540. | 1383 | 790. | 1761 |
| 550. | 1392 | 800. | 1779 |
| 560. | 1400 | 810. | 1798 |
| 570. | 1409 | 820. | 1816 |
| 580. | 1419 | | |
| 590. | 1430 | | |

$$ {}^{a}C_S^o(\theta) = {}^{a}C_S^o(296K) \exp\left(\frac{b}{\theta} - \frac{b}{296}\right) $$

TABLE 5

EMPIRICAL $H_2O$ CONTINUUM COEFFICIENT
FOR SELF-BROADENING AT DIFFERENT TEMPERATURES.

Multiply all values by $10^{-24}$ molecules$^{-1}$ cm$^2$ atm$^{-1}$

| $\nu$ cm$^{-1}$ | 200K | 210K | 220K | 230K | 240K | 250K | 260K | 270K |
|---|---|---|---|---|---|---|---|---|
| 320. | 83716. | 62942. | 48567. | 38329. | 30852. | 25268. | 21015. | 17719. |
| 330. | 78421. | 58843. | 45320. | 35707. | 28697. | 23471. | 19495. | 16417. |
| 340. | 73458. | 55008. | 42290. | 33264. | 26693. | 21800. | 18084. | 15211. |
| 350. | 68809. | 51423. | 39461. | 30987. | 24828. | 20249. | 16775. | 14093. |
| 360. | 64460. | 48076. | 36825. | 28869. | 23095. | 18809. | 15563. | 13058. |
| 370. | 60381. | 44943. | 34363. | 26894. | 21482. | 17471. | 14436. | 12099. |
| 380. | 56564. | 42017. | 32067. | 25055. | 19983. | 16229. | 13392. | 11210. |
| 390. | 52983. | 39278. | 29922. | 23340. | 18586. | 15073. | 12423. | 10386. |
| 400. | 49635. | 36722. | 27923. | 21745. | 17290. | 14002. | 11525. | 9624. |
| 410. | 46492. | 34328. | 26055. | 20256. | 16081. | 13005. | 10690. | 8916. |
| 420. | 43549. | 32090. | 24312. | 18869. | 14958. | 12079. | 9917. | 8261. |
| 430. | 40800. | 30004. | 22690. | 17581. | 13915. | 11222. | 9200. | 7655. |
| 440. | 38213. | 28045. | 21170. | 16376. | 12941. | 10422. | 8533. | 7092. |
| 450. | 35798. | 26220. | 19756. | 15256. | 12038. | 9681. | 7916. | 6571. |
| 460. | 33536. | 24514. | 18437. | 14214. | 11199. | 8993. | 7344. | 6089. |
| 470. | 31411. | 22915. | 17203. | 13240. | 10416. | 8352. | 6812. | 5641. |
| 480. | 29421. | 21420. | 16051. | 12333. | 9687. | 7757. | 6319. | 5226. |
| 490. | 27564. | 20027. | 14980. | 11491. | 9012. | 7206. | 5862. | 4843. |
| 500. | 25819. | 18722. | 13978. | 10705. | 8382. | 6693. | 5438. | 4487. |
| 510. | 24184. | 17501. | 13043. | 9972. | 7796. | 6217. | 5044. | 4157. |
| 520. | 22655. | 16362. | 12171. | 9290. | 7252. | 5775. | 4680. | 3852. |
| 530. | 21219. | 15294. | 11356. | 8653. | 6745. | 5363. | 4340. | 3568. |
| 540. | 19880. | 14300. | 10599. | 8063. | 6275. | 4983. | 4027. | 3307. |
| 550. | 18625. | 13370. | 9891. | 7512. | 5837. | 4629. | 3736. | 3064. |
| 560. | 17447. | 12499. | 9230. | 6998. | 5430. | 4299. | 3466. | 2839. |
| 570. | 16342. | 11684. | 8612. | 6519. | 5050. | 3993. | 3215. | 2630. |
| 580. | 15405. | 10988. | 8081. | 6105. | 4721. | 3726. | 2995. | 2447. |
| 590. | 14586. | 10376. | 7613. | 5738. | 4428. | 3489. | 2800. | 2284. |
| 600. | 13860. | 9832. | 7196. | 5411. | 4167. | 3277. | 2625. | 2137. |
| 610. | 13221. | 9351. | 6825. | 5120. | 3934. | 3087. | 2468. | 2006. |
| 620. | 12660. | 8926. | 6497. | 4862. | 3727. | 2918. | 2328. | 1889. |
| 630. | 12180. | 8560. | 6213. | 4636. | 3545. | 2770. | 2205. | 1786. |
| 640. | 11752. | 8232. | 5956. | 4432. | 3380. | 2635. | 2093. | 1692. |
| 650. | 11378. | 7942. | 5728. | 4250. | 3233. | 2513. | 1992. | 1607. |
| 660. | 11074. | 7701. | 5535. | 4094. | 3106. | 2408. | 1905. | 1533. |
| 670. | 10823. | 7496. | 5368. | 3958. | 2993. | 2314. | 1825. | 1465. |
| 680. | 10633. | 7333. | 5230. | 3842. | 2896. | 2232. | 1756. | 1406. |
| 690. | 10461. | 7182. | 5103. | 3735. | 2806. | 2156. | 1691. | 1351. |
| 700. | 10282. | 7029. | 4974. | 3628. | 2716. | 2081. | 1628. | 1296. |
| 710. | 10110. | 6881. | 4851. | 3525. | 2630. | 2009. | 1567. | 1245. |
| 720. | 9932. | 6731. | 4726. | 3422. | 2545. | 1938. | 1508. | 1195. |
| 730. | 9764. | 6589. | 4609. | 3324. | 2464. | 1871. | 1451. | 1147. |
| 740. | 9593. | 6445. | 4489. | 3227. | 2384. | 1805. | 1396. | 1100. |
| 750. | 9432. | 6310. | 4378. | 3136. | 2309. | 1743. | 1344. | 1057. |
| 760. | 9270. | 6174. | 4267. | 3045. | 2235. | 1682. | 1293. | 1014. |
| 770. | 9122. | 6049. | 4164. | 2961. | 2166. | 1625. | 1246. | 975. |
| 780. | 8956. | 5914. | 4055. | 2873. | 2095. | 1567. | 1198. | 935. |
| 790. | 8808. | 5790. | 3954. | 2792. | 2029. | 1513. | 1154. | 898. |
| 800. | 8660. | 5668. | 3856. | 2712. | 1965. | 1460. | 1111. | 862. |
| 810. | 8514. | 5549. | 3760. | 2635. | 1902. | 1410. | 1069. | 827. |
| 820. | 8370. | 5431. | 3666. | 2560. | 1842. | 1361. | 1029. | 795. |

(cont.)

TABLE 5 (cont.)

EMPIRICAL $H_2O$ CONTINUUM COEFFICIENT
FOR SELF-BROADENING AT DIFFERENT TEMPERATURES.

| $\nu$ $cm^{-1}$ | Multiply all values by $10^{-24}$ $molecules^{-1}$ $cm^2$ $atm^{-1}$ | | | | | | | |
|---|---|---|---|---|---|---|---|---|
| | 280K | 290K | 296K | 300K | 310K | 320K | 338K | 430K |
| 320. | 15122. | 13048. | 12000. | 11370. | 9996. | 8859. | 7257. | 3400. |
| 330. | 13996. | 12063. | 11088. | 10502. | 9224. | 8168. | 6682. | 3114. |
| 340. | 12953. | 11153. | 10245. | 9699. | 8512. | 7531. | 6152. | 2852. |
| 350. | 11987. | 10311. | 9466. | 8959. | 7854. | 6943. | 5664. | 2611. |
| 360. | 11095. | 9533. | 8747. | 8275. | 7248. | 6402. | 5216. | 2392. |
| 370. | 10268. | 8814. | 8082. | 7643. | 6689. | 5903. | 4802. | 2190. |
| 380. | 9504. | 8149. | 7468. | 7060. | 6173. | 5443. | 4421. | 2006. |
| 390. | 8795. | 7534. | 6900. | 6520. | 5696. | 5018. | 4071. | 1837. |
| 400. | 8140. | 6966. | 6376. | 6023. | 5256. | 4627. | 3748. | 1682. |
| 410. | 7534. | 6440. | 5891. | 5562. | 4850. | 4266. | 3451. | 1541. |
| 420. | 6972. | 5953. | 5443. | 5137. | 4476. | 3933. | 3177. | 1411. |
| 430. | 6453. | 5505. | 5030. | 4746. | 4131. | 3627. | 2926. | 1292. |
| 440. | 5972. | 5089. | 4647. | 4383. | 3811. | 3343. | 2693. | 1183. |
| 450. | 5527. | 4705. | 4294. | 4048. | 3517. | 3083. | 2480. | 1084. |
| 460. | 5116. | 4350. | 3968. | 3740. | 3246. | 2843. | 2284. | 993. |
| 470. | 4734. | 4022. | 3666. | 3454. | 2995. | 2621. | 2102. | 909. |
| 480. | 4381. | 3718. | 3387. | 3190. | 2764. | 2416. | 1935. | 832. |
| 490. | 4055. | 3438. | 3130. | 2946. | 2551. | 2228. | 1782. | 762. |
| 500. | 3753. | 3178. | 2892. | 2721. | 2354. | 2054. | 1641. | 698. |
| 510. | 3473. | 2938. | 2672. | 2513. | 2172. | 1894. | 1511. | 639. |
| 520. | 3215. | 2717. | 2469. | 2322. | 2004. | 1746. | 1391. | 586. |
| 530. | 2975. | 2511. | 2281. | 2144. | 1849. | 1610. | 1280. | 536. |
| 540. | 2754. | 2322. | 2108. | 1981. | 1707. | 1485. | 1179. | 491. |
| 550. | 2549. | 2147. | 1948. | 1830. | 1575. | 1369. | 1086. | 450. |
| 560. | 2359. | 1985. | 1800. | 1690. | 1454. | 1262. | 1000. | 412. |
| 570. | 2183. | 1835. | 1663. | 1561. | 1341. | 1164. | 920. | 377. |
| 580. | 2028. | 1703. | 1542. | 1446. | 1242. | 1076. | 850. | 346. |
| 590. | 1890. | 1585. | 1434. | 1345. | 1153. | 998. | 787. | 318. |
| 600. | 1766. | 1479. | 1337. | 1253. | 1073. | 928. | 730. | 293. |
| 610. | 1655. | 1384. | 1250. | 1171. | 1001. | 865. | 679. | 270. |
| 620. | 1556. | 1299. | 1172. | 1097. | 937. | 808. | 633. | 250. |
| 630. | 1468. | 1223. | 1103. | 1032. | 880. | 758. | 592. | 232. |
| 640. | 1388. | 1155. | 1040. | 972. | 828. | 712. | 555. | 215. |
| 650. | 1316. | 1092. | 983. | 918. | 781. | 670. | 521. | 200. |
| 660. | 1253. | 1038. | 933. | 871. | 739. | 634. | 492. | 187. |
| 670. | 1195. | 988. | 887. | 827. | 701. | 600. | 464. | 175. |
| 680. | 1144. | 944. | 846. | 789. | 667. | 570. | 439. | 164. |
| 690. | 1096. | 902. | 808. | 753. | 635. | 542. | 416. | 153. |
| 700. | 1050. | 862. | 771. | 717. | 604. | 514. | 394. | 143. |
| 710. | 1005. | 824. | 736. | 684. | 575. | 489. | 374. | 134. |
| 720. | 962. | 787. | 702. | 652. | 547. | 464. | 354. | 126. |
| 730. | 922. | 752. | 670. | 622. | 521. | 441. | 335. | 118. |
| 740. | 882. | 718. | 639. | 593. | 495. | 418. | 317. | 110. |
| 750. | 845. | 686. | 610. | 565. | 471. | 398. | 300. | 103. |
| 760. | 809. | 656. | 582. | 539. | 449. | 378. | 284. | 96. |
| 770. | 776. | 627. | 556. | 514. | 427. | 359. | 269. | 90. |
| 780. | 742. | 599. | 530. | 490. | 406. | 341. | 255. | 85. |
| 790. | 711. | 572. | 506. | 467. | 387. | 324. | 242. | 79. |
| 800. | 681. | 547. | 483. | 446. | 368. | 308. | 229. | 74. |
| 810. | 652. | 523. | 461. | 425. | 350. | 292. | 217. | 69. |
| 820. | 625. | 500. | 440. | 405. | 333. | 278. | 205. | 65. |

TABLE 6

EMPIRICAL $H_2O$ CONTINUUM COEFFICIENT[(a)] FOR $N_2$-BROADENING

| $\nu$ ($cm^{-1}$) | $^aC_N^o$ (a) | $\nu$ ($cm^{-1}$) | $^aC_N^o$ (a) | $\nu$ ($cm^{-1}$) | $^aC_N^o$ (a) | $\nu$ ($cm^{-1}$) | $^aC_N^o$ (a) |
|---|---|---|---|---|---|---|---|
| | | 400 | 53.2 | 500 | 24.2 | 600 | 11.8 |
| | | 410 | 47.5 | 510 | 23.1 | 610 | 10.6 |
| 320 | 1120 | 420 | 42.5 | 520 | 22.0 | 620 | 9.3 |
| 330 | 602 | 430 | 38.5 | 530 | 20.7 | 630 | 8.0 |
| 340 | 374 | 440 | 35.0 | 540 | 19.4 | 640 | 6.7 |
| 350 | 244 | 450 | 32.6 | 550 | 18.1 | | |
| 360 | 163 | 460 | 30.3 | 560 | 16.9 | | |
| 370 | 113 | 470 | 28.4 | 570 | 15.6 | | |
| 380 | 84.2 | 480 | 26.7 | 580 | 14.4 | | |
| 390 | 68.0 | 490 | 25.7 | 590 | 13.1 | | |

(a) The units for the empirical continuum coefficient are molecules $^{-1}$ $cm^2$ $atm^{-1}$. The values must be multiplied by $10^{-24}$.

TABLE 7

ATTENUATION COEFFICIENT
FOR $H_2O$ EMPIRICAL CONTINUUM FOR
THREE ATMOSPHERIC CONDITIONS

| | | | |
|---|---|---|---|
| θ(K) | 296 | 240 | 240 |
| p(atm) | 0.0277 | 0.00032 | 0.00032 |
| P(atm) | 1.00 | 1.00 | 0.306 |
| (a) u(#/cm²) | 6.89 E20 | 9.78 E18 | 9.78 E18 |
| ν (cm⁻¹) | $\beta_L$ (km⁻¹) | $\beta_L$ (km⁻¹) | $\beta_L$ (km⁻¹) |
| 320. | 0.97853 | 0.01105 | 0.00345 |
| 330. | 0.61443 | 0.00598 | 0.00189 |
| 340. | 0.44574 | 0.00374 | 0.00120 |
| 350. | 0.34387 | 0.00246 | 0.00081 |
| 360. | 0.27594 | 0.00167 | 0.00056 |
| 370. | 0.22979 | 0.00117 | 0.00041 |
| 380. | 0.19880 | 0.00089 | 0.00031 |
| 390. | 0.17713 | 0.00072 | 0.00026 |
| 400. | 0.15723 | 0.00057 | 0.00021 |
| 410. | 0.14416 | 0.00051 | 0.00019 |
| 420. | 0.13227 | 0.00046 | 0.00017 |
| 430. | 0.12171 | 0.00042 | 0.00016 |
| 440. | 0.11206 | 0.00038 | 0.00015 |
| 450. | 0.10372 | 0.00036 | 0.00014 |
| 460. | 0.09597 | 0.00033 | 0.00013 |
| 470. | 0.08893 | 0.00031 | 0.00012 |
| 480. | 0.08248 | 0.00029 | 0.00011 |
| 490. | 0.07690 | 0.00028 | 0.00011 |
| 500. | 0.07136 | 0.00026 | 0.00010 |
| 510. | 0.06643 | 0.00025 | 0.00009 |
| 520. | 0.06182 | 0.00024 | 0.00009 |
| 530. | 0.05736 | 0.00022 | 0.00008 |
| 540. | 0.05319 | 0.00021 | 0.00008 |
| 550. | 0.04927 | 0.00020 | 0.00007 |
| 560. | 0.04565 | 0.00018 | 0.00007 |
| 570. | 0.04216 | 0.00017 | 0.00006 |
| 580. | 0.03905 | 0.00016 | 0.00006 |
| 590. | 0.03612 | 0.00014 | 0.00005 |
| 600. | 0.03340 | 0.00013 | 0.00005 |
| 610. | 0.03094 | 0.00012 | 0.00004 |
| 620. | 0.02858 | 0.00010 | 0.00004 |
| 630. | 0.02639 | 0.00009 | 0.00004 |
| 640. | 0.02432 | 0.00008 | 0.00003 |

(a)The unit molecules/cm² is abbreviated by #/cm²
The value of u corresponds to a 1-km path.

T (empirical continuum) = $\exp(-\beta_L L)$

## SECTION 6

## REFERENCES


1. Darrell E. Burch, David A. Grynvak, and Francis J. Gates; "Continuum Absorption by $H_2O$ Between 330 and 825 $cm^{-1}$", Final Report No. AFCRL-TR 74-0377 on Contract No. F19628-74-C-0069. Aeronutronic Report No. U-6095 September 1974

2. Darrell E. Burch, David A. Gryvnak, and John D. Pembrook; "Infrared Absorption by $H_2O$, NO and $N_2O$", Final Report No. AFCRL-TR-75-0420 on Contract No. F19628-75-C-0049. Aeronutronic Report No. U-6159, September 1975.

3. David A. Gryvnak, Darrell E. Burch, Robert L. Alt, and Dorianne K. Zgonc; "Infrared Absorption by $CH_4$, $H_2O$ and CO", Final Report No. AFGL-TR-76-0246 on Contract F19628-76-C-0067. Aeronutronic Report No. U-6275, December 1977.

4. David A. Gryvnak and Darrell E. Burch, "Infrared Absorption by CO and $N_2O$. Scientific Report AFGL-TR-78-0154. Aeronutronic Report No. U-6417, May 1978.

5. R. A. McClatchey, W.S. Benedict, S.A. Clough, D. E. Burch, R. F. Calfee, K. Fox, L.S. Rothman, and J.S. Garing; "AFCRL Atmospheric Absorption Line Parameters Compilation", AFCRL-TR-73-0096, 26 January 1973. (Associated with this report is a magnetic tape listing the line parameters.)

6. C.H. Palmer Jr., J. Opt. Soc. Am. 50, 1232 (1960).

7. K.J. Bignell, Quart J. Roy. Met. Soc. 96, 390 (1970).

8. Darrell E. Burch, David A. Grynvak, R. R. Patty and C.E. Bartky, J.Opt. Soc.Am. 59, 267 (1969).

9. B. H. Winters, S. Silverman, and W.S. Benedict, J.Quant. Spectry Radiative Transfer 4, 527 (1964).

10. Darrell E. Burch, David A. Gryvnak, and R. R. Patty, "Absorption of Infrared Ratiation by CO and $H_2O$. I. Experimental Techniques," J.Opt.Soc. Am. 57 885 (1967 ).

11. Darrell E. Burch, "Investigation of the Absorption of Infrared Radiation by Atmospheric Gases." Semi-Annual Technical Report, Contract F19628-69-C-0263. Aeronutronic Report No. U-4784, January 1970.

12. R. E. Robert, J.E.A. Selby, and L.M. Biberman, Appl. Opt. 15, 2085 (1967).

13. Darrell E. Burch, David A. Gryvnak, and John D. Pembrook, "Investigation of the Absorption by Atmospheric Gases" Water, Nitrogen, Nitrous Oxide Semi-Annual Technical Report No. 2 AFCRL-71-0124. Aeronutronic Report No. U-4897 January 1971

14. R.A. McClatchey, R.W. Fenn, J.E.A. Selby, F.E. Volz, and J.S. Garing "Optical Properties of the Atmosphere (Third Edition) Report No. AFCRL-72-0497,